SANDIA REPORT
SAND2018-8192
Printed August 2018

Deposition Velocity Modeling for Turbo FRMAC

John D. Fulton

Prepared by
Sandia National Laboratories
Albuquerque, New Mexico 87185 and Livermore, California 94550

Sandia National Laboratories is a multimission laboratory managed and operated by National Technology & Engineering Solutions of Sandia, LLC, a wholly owned subsidiary of Honeywell International Inc., for the U.S. Department of Energy's National Nuclear Security Administration under contract DE-NA0003525.

Further dissemination authorized to the Department of Energy and DOE contractors only; other requests shall be approved by the originating facility or higher DOE programmatic authority.

Issued by Sandia National Laboratories, operated for the United States Department of Energy by Sandia Corporation.

NOTICE: This report was prepared as an account of work sponsored by an agency of the United States Government. Neither the United States Government, nor any agency thereof, nor any of their employees, nor any of their contractors, subcontractors, or their employees, make any warranty, express or implied, or assume any legal liability or responsibility for the accuracy, completeness, or usefulness of any information, apparatus, product, or process disclosed, or represent that its use would not infringe privately owned rights. Reference herein to any specific commercial product, process, or service by trade name, trademark, manufacturer, or otherwise, does not necessarily constitute or imply its endorsement, recommendation, or favoring by the United States Government, any agency thereof, or any of their contractors or subcontractors. The views and opinions expressed herein do not necessarily state or reflect those of the United States Government, any agency thereof, or any of their contractors.

SAND2018-8192
Printed August 2018

Deposition Modeling for Turbo FRMAC

John D. Fulton
System Research and Analysis (8852)
Sandia National Laboratories
P. O. Box 5800
Albuquerque, New Mexico 87185-MS0748

Abstract

The Federal Radiological Monitoring and Assessment Center (FRMAC) has two major assets it uses to perform it responsibilities for responding to a radiological emergency. These are the National Atmospheric Release Advisory Capability (NARAC) and Turbo FRMAC. Recently NARAC updated their deposition model to the state of the art Petroff and Zhang model leading to a significant discrepancy between these two assets in regards to deposition modeling. This report describes the investigation into an appropriate deposition model for Turbo FRMAC to bring the two assets back into line. The ultimate conclusion is that Petroff and Zhang is too complicated for Turbo FRMAC, but the model of Feng is not and is equal to Petroff and Zhang in predictive capability.

Further dissemination authorized to the Department of Energy and DOE contractors only; other requests shall be approved by the originating facility or higher DOE programmatic authority.

ACKNOWLEDGMENTS

The author would like to thank Dan Blumenthal of DOE NA-84 for funding this work through the FEMA-NIRT process. The author would also like to thank Terry Kraus and Lainy Cochran for serving as reviewer of this paper. The author would also like to thank Johann Synder for his assistance in editing and formatting this document.

TABLE OF CONTENTS

FIGURES

TABLES

EXECUTIVE SUMMARY

The Federal Radiological Monitoring and Assessment Center (FRMAC) relies on two key assets to make assessments of radiological impact during and emergency. They are the National Atmospheric Release Advisory Capability (NARAC), and the Consequence Home Team (CMT) which uses the Turbo FRMAC software. NARAC is used to predictively model the atmospheric dispersion of material while Turbo FRMAC is used to calculate emergency response values based on in situ field measurements or predictive assumption on the released mix of radionuclides.

Currently there is a substantial gap in the assumption of a critical parameter known as the deposition velocity. Deposition velocity is used by the NARAC model to determine the amount of material that should be deposited on the ground based on air concentrations, while it is used in Turbo FRMAC to calculate either deposition or air concentration from the other if one of the two values is not known. The gap in deposition velocity is this: NARAC uses a state-of-the-art model to predict the deposition of material to the ground from the air which takes into account the critical aspects of friction velocity and particle size on deposition, while Turbo FRMAC uses historical constant values that ignore all aspects that are critical to determination of deposition velocity. Thus, even with identical air concentration and/or deposition data, the two assets can determine substantially different impacts.

The purpose of this report is to describe the literature review that was performed on behalf of the CMT in order to determine the appropriate deposition model for Turbo FRMAC that would align and modernize it consistent with NARAC. In this report, a general discussion of the concept of deposition velocity is given, including a discussion of the critical parameters that are necessary to accurately calculate the value. Then the report notes that deposition models can be broken down into two main families of models. Those patterned after the work of Sehmel[1], and those patterned off the work of Slinn and Slinn[2].

Next the report describes models from both of the two families of deposition models and provides discussion on the pros and cons. Ultimately recommending a “best of breed” model from both families. For the Sehmel family this is the model of Feng[3], whereas for the Slinn and Slinn family it is the model of Petroff and Zhang[4]. As part of this comparison, a discussion on data used to derive the models is also included so as to understand the quality of the underlying data and assumptions.

---

[1] Sehmel, G. A., & Hodgson, W. H. (1978). *A Model for Predicting Dry Deposition of Particles and Gases to Environment Surfaces - PNL-SA-6721.* Richland: Battelle-Pacific Northwest Laboratories.

[2] Slinn, S. A., & Slinn, W. G. (1980). “Predictions for Particle Deposition on Natural Waters”. *Atmospheric Environment, 14*, 1013-1016

[3] Feng, J. (2008). “A Size-Resolved Model and a Four-Mode parameterization of Dry Deposition of Atmospheric Aerosols”. *Journal of Geophysical Research, 113*, D12201-

[4] Petroff, A., & Zhang, L. (2010). “Development and Validation of a Size-Resolved Particle Dry Deposition Scheme For Applications in Aerosol Transport Models”. *Geoscience Model Development Discussions, 3*, 1317-1357

After this a discussion ensues on NARAC's decision to use the model of Petroff and Zhang and why this choice is eminently reasonable for the environment in which NARAC operates but unfeasible for Turbo FRMAC. Thus, a section follows in which the "best of breed" Petroff and Zhang model and the model of Feng are compared. Ultimately, it is not only shown that the model of Feng is more appropriate to the operational conditions under which Turbo FRMAC is used, but also that the model of Feng shows predictive superiority to the model of Petroff and Zhang. However, it is also noted that Petroff and Zhang and Feng agree sufficiently with each other that implementation of the one by NARAC and the other by Turbo FRMAC will still eliminate the present gap and discrepancy between the two codes.

Therefore, this report concludes by determining that the model of Feng should be used by Turbo FRMAC. In this recommendation it further provides a proposed implementation of Feng for Turbo FRMAC that will allow the use of Feng in either a detailed model or the situation of no knowledge regarding atmospheric conditions.

NOMENCLATURE

Abbreviation	Definition
FRMAC	Federal Radiological Monitoring and Assessment Center
NARAC	National Atmospheric Release Advisory Center
AHT	Assessment Home Team
CHT	Consequence Home Team
NOAA	National Oceanic and Atmospheric Administration
HYSPLIT	Hybrid Single Particle Lagrangian Integrated Trajectory
WRF	Weather Researching and Forecast
LAI	Leaf Area Index

Page Intentionally Blank

1. INTRODUCTION

During a response to a radiological emergency the Federal Radiological Monitoring and Assessment Center (FRMAC) uses several assets and tools to respond to an emergency. One of those assets is National Atmospheric Release Advisory Center (NARAC) and its atmospheric transport models, and the other is the Assessment Home Team (AHT) which uses the Turbo FRMAC software. The NARAC model is used to transport an assumed source term of radioactive material using observed and forecast meteorological conditions through the atmosphere. This is done to predict potential air concentrations and ground deposition values. Meanwhile, Turbo FRMAC is used, either with the same assumed source term or using field samples of airborne concentration and/or ground concentration, to calculate threshold values of interest for evacuation, sheltering, food embargo, etc.

For both tools the concept of dry deposition is important. The NARAC model is transporting material over local, regional, and global scales depending on the situation, and needs to model the deposition of material from the air to the surface over such scales. To do so it needs availability to terrain, roughness, and landuse databases, as well as meteorological conditions over these scales. These datasets are necessary to properly transport and deposit material to the ground from the air as they are transported by the prevailing meteorological conditions. The situation for Turbo FRMAC is ultimately quite different as Turbo FRMAC is essentially a point model, using conditions at a specific point in space and time to calculate relevant values. An essential aspect to many of these calculations is the availability of both integrated air and ground concentrations of material. Often only one of these values is known (or assumed) and the other is inferred from the known value. The value that enables this is the so called "deposition velocity".

In Turbo FRMAC, deposition velocity is treated as a constant value of 0.3 cm s^{-1} (0.0 for many gasses, and 0.65 for Iodines) which is very close to the traditional value of 0.1 cm s^{-1} used by air quality models that do not have the sophistication of the NARAC model or the National Oceanic and Atmospheric Administration's (NOAA) Hybrid Single Particle Lagrangian Integrated Trajectory (HYSPLIT) model[5]. As noted by Hicks[6], the origin of these traditional values is uncertain and questionable, with many studies indicating deposition velocities in excess of 1 cm s^{-1}, even for gases[7,8]. Hence, an updated and defensible deposition model is needed for Turbo FRMAC.

The purpose of this report is to present a basic understanding of the meaning of deposition velocity, describe a series of available deposition models and their limitations, and then recommend a path forward for implementing deposition in a

[5] Stein, A. D. (2015). "NOAA's HYSPLIT atmospheric transport and dispersion modeling system". *Bulletin of the American Meteorological Society*, 96, 2059-2077.

[6] Hicks, B. B., Saylor, R. D., Baker, B. D., & . (2016). "Dry Deposition of Particles to Canopies-A Look Back and the Road Forward". *Journal of Geophysical Research: Atmospheres*, 14691-14707.

[7] Ruijgrok, W., Tieben, H., Eisinga, P., & . (1997). "The Dry Deposition of Particles to a Forest Canopy: A Comparison of Model and Experimental Results". *Atmospheric Environment, 31*(3), 399-415

[8] Wu, Y.-L., Davidson, C. I., Dolske, D. A., & Sherwood, S. I. (1992). "Dry Deposition of Atmospheric Contaminants: The Relative Importance of Aerodynamic, Boundary Layer, and Surface Resistances". *Aerosol Science and Technology*, 16, 65-81

more consistent manner between NARAC and Turbo FRMAC. The remainder of this report is thus broken down in the following manner.

First the term deposition velocity is described in general. This is further broken down to a discussion of key factors affecting deposition, and important model limitations. Next, a section is dedicated to describing the two main families of deposition models along with key models within each family. These two families are then compared. Finally, the current NARAC solution and the proposed path forward are discussed before final conclusions.

2. DEPOSITION VELOCITY

In this section a general overview of the concept of deposition velocity is provided. This includes a general discussion of the concept, followed by an overview of key factors affecting deposition velocity. Finally, a summary section highlights key takeaways for the rest of the report.

2.1. General Discussion

Dry deposition is the depositing of material in the air to the ground via mechanism that do not include removal by precipitation (wet deposition). It is usually described as the ratio of the dry deposition flux (mass per time per area[2] ($g\ s^{-1}\ m^{-2}$)) to the air concentration (mass per volume ($g\ m^{-3}$)) above the surface where the deposition velocity is to be calculated. Since this ratio has units of $m\ s^{-1}$ it is commonly referred to as the dry deposition velocity[9] and given the symbol V_d or v_d. Mathematically this term is:

* MERGEFORMAT [2.1]

$$V_d = \frac{DepositionFlux}{AirConcentration} = \frac{\frac{g}{s*m^2}}{\frac{g}{m^3}} = \frac{m}{s}$$

Or

* MERGEFORMAT [2.2]

$$V_d = \frac{GroundConcentration}{IntegratedAirConcentration} = \frac{\frac{g}{m^2}}{\frac{g*s}{m^3}} = \frac{m}{s}$$

where the * MERGEFORMAT [2.2] is what is more typically measured.

As noted, the name of this ratio is the dry deposition velocity or simple the deposition velocity. This name is most unfortunate as its implies that all material on the ground was deposited from material in the air . The name thus does not allow for any a priori concentration of the measured contaminant on the ground, or ingrowth of the contaminant from another contaminant species already on the ground. Furthermore, it assumes material is flowing purely in a downward direction at a fixed speed, but in reality, this term represents the combined effect of all processes that contribute to deposition[10], which can include processes such as: resuspension which is essentially negative deposition, emission for sources below the level at which air concentration was measure, etc. Finally, the process of deposition can be highly chaotic and driven by turbulent bursts[11] and thus is not necessarily well represented by a constant deposition velocity.

---

[9] Feng, J. (2008). "A Size-Resolved Model and a Four-Mode Parameterization of Dry Deposition of Atmospheric Aerosols". *Journal of Geophysical Research, 113*, D12201.

[10] Sehmel, G. A. (1973). "Particle Eddy Diffusivities and Deposition Velocities for Isothermal Flow and Smooth Surfaces". *Aerosol Science, 4*, 125-138.

[11] (Feng, 2008)

As noted by Sehmel[12], "the K [deposition velocity] then are also a function of particle reentrainment or accommodation coefficient. Since the resultant forces of these individual forces cannot be predicted for turbulent flow, reported K values describe the total effect of all forces which have not been minimized by the selected experimental conditions". In this statement Sehmel makes an important warning to anyone investigating deposition velocity that they must fully understand those factors that are, and are not accounted for by the experiment, and understand how they greatly impact the meaning and ability to compare deposition velocities from one paper to another.

The equation that is used to calculate deposition velocity has many implied assumptions. The first of these has already been noted, it is that all material on the ground came from the air.

The second is that air concentration is constant from the reference height at which it is measured to the ground. Thus, the value of deposition velocity is dependent on the reference height at which measurements are made, making deposition velocity a function of height[13]. This is easy to visualize if one considers a column of air with constant concentration from the ground to a reference height. If any of the contaminant deposits on the ground the concentration is reduced just above the ground producing a gradient of lower concentration to higher. Material through diffusional processes will then begin to migrate down gradient to the zone of lower concentration creating a vertical concentration profile. Since surfaces available for contaminant removal also tend to increase as material gets closer to the ground these two processes naturally produce a profile of ever increasing concentration up to some reference or source emission height. Thus, measuring the air concentration at ever increasing height will produce higher deposition velocities than air concentrations measured near the ground given the same measured ground concentration.

A third assumption in the definition of deposition velocity is the assumption of steady-state conditions. However, deposition velocities are known to decrease versus time as material concentrations in the air reduce due to deposition before ultimately reaching a quasi-steady-state[14].

Sehmel[15] comments on assumptions two and three when he says, "There is a fallacy in this deposition velocity concept. It is the exception, rather than the rule that nonsteady-state mass transfer can be adequately described by a single point concentration measurement. If mass transfer occurs, a profile of airborne concentration versus height must develop to act as the driving gradient for mass transfer in a diffusion-controlled process." He further comments that, "We must remember that even with a relative insensitivity to height at 1 m, deposition velocities are only an approximation to describe the unsteady state diffusion-transport boundary limits."

---

[12] Sehmel, G. A. (1971). "Particle Diffusivities and Deposition Velocities over a Horizontal Smooth Surface". *Journal of Colloid and Interface Science, 37*(4), 891-906

[13] (Sehmel, Particle Diffusivities and Deposition Velocities over a Horizontal Smooth Surface, 1971)

[14] (Wu, Davidson, Dolske, & Sherwood, 1992)

[15] Sehmel, G. A., & Hodgson, W. H. (1978). *A Model for Predicting Dry Deposition of Particles and Gases to Environment Surfaces - PNL-SA-6721.* Richland: Battelle-Pacific Northwest Laboratories.

These statements by Sehmel are critical to understanding the ultimate conclusions of this report and the limitations of any deposition report available in the literature. All are making the assumption that air concentration values are horizontally and vertically homogenous from the measurement height to the ground. All are eliminating any form of resuspension; material flows down, not up. Most further assume temporal homogeneity for at least some duration which is typically 30 minutes[16]. This strictly speaking is a fallacy. Material is not homogeneous; it does not deposit steadily, but in bursts; it does resuspend; and the measurement height of the air concentration is critical. Furthermore, the deposition velocity value is not a velocity, it is purely a scalar constant that requires units of m s^{-1} to relate an integrated airborne concentration to a ground concentration, two values that may not actually be correlated.

2.2. Key Factors

There are numerous factors that control the deposition of material from the air to the ground. Figure 1 is a reproduction of Figure 5 from (Hicks, Saylor, & Baker, 2016) which lists all the current processes known in some way and in some situations to impact deposition of particles and gases. Each of these will be described briefly before highlighting those factors that have been found to be most essential. Note that in Figure 1, the dotted box is turbophoresis, which is a factor that has not received much attention historically and will be shown later to be a great significance.

[16] Gallagher, M. W., Beswick, K. M., Duyzer, J., Westrate, H., Choularton, T. W., & Hummelshoj, P. (1997). "Measurement of Aerosol Fluxes to Speulder Forest Using a Micrometeorological Technique". *Atmospheric Environment, 31*(3), 359-373

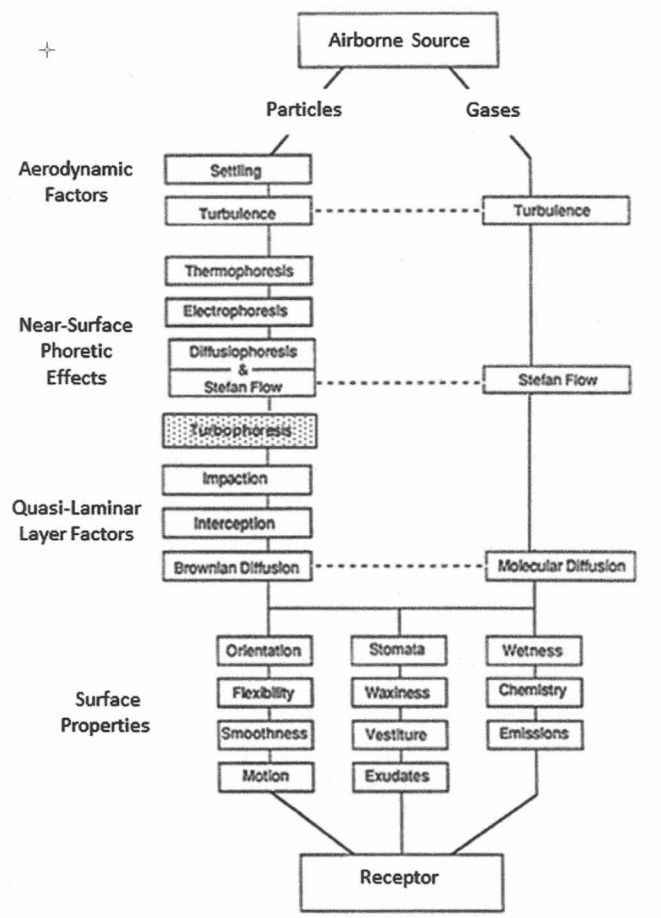

Figure 1: Reproduction of Figure 5 from (Hicks, Saylor, & Baker, 2016).

The first process noted is settling, or better known as gravitational settling. This process represents the terminal velocity a particle reaches as it falls under the influence of gravity and drag.

The second process is turbulence and represents the movement of gasses and particles due to atmospheric turbulent eddies.

Process one and two are the driving processes governing the deposition of large particles.

The third process, thermophoresis, is the first of the phoretic effects (movement from one location to another by a process or carrier). Thermophoresis is the process of particles migrating away from a hot surface due to higher energy gas molecules emanating from the hot surface imparting more momentum away from the surface than the momentum imparted by cooler molecules farther way from the surface towards the surface.

The fourth process is electrophoresis, which is the attraction of charged particles to surfaces due to the electric potential of the surface. This process is a strong function of particle size and likely only significant to smaller particles.

The fifth process is diffusiophoresis which is the process by which particulate or gases are moved in the direction of lower concentration of another species. A typical example is water vapor where high surface concentrations due to evaporation are pushing particulates away from the surface as the water vapor flows past from its zone of higher concentration to lower concentration.

The sixth process, Stefan Flow, is similar to diffusiophoresis in that it is motion away from a surface caused when material in one form (liquid) become a gas, a process that displaces a large volume of gas above the surface even when only a small volume of liquid evaporates. This displacement of gas away from the surface thus imparts a velocity to any particulate above the surface.

The seventh process is turbophoresis. Turbophoresis derives from the inability of particles to respond quickly to turbulent fluctuations near a surface, the net effect being that particles are transported to areas of lower turbulent kinetic energy and thus towards any available surface.

All of the phoretic processes are processes which are typically important for smaller particles.

The seventh process is impaction and it occurs when particles have sufficient mass they cannot bend with the streamlines around an object and impact the surface.

The eight process is interception and it occurs when particles are able to bend with the streamlines around a surface but they still come within one particle radius or less to the surface and thus intercept the surface and are bound to it.

Interception and impaction are important to intermediate size particles and their range of influence shifts to smaller particles as wind velocities increase and towards larger particles as wind velocities slow.

The ninth process is Brownian diffusion which dominates only the smallest of particles and is critical to deposition by gases.

The last process is not truly a process, but a collection of various aspects of the surface on which deposition is occurring that influence interception and impaction. Key features include: orientation to the flow (is the branch along or broadside to the flow), flexibility (can the leaf bend into an orientation along the flow), smoothness (leaf hairs matter), motion (swaying grass), stomata (open or close affects phoretic effects), waxiness (do particles stick, bounce, or slide off), vestiture (what coats the surface), exudates (leaf exudes an oil, etc.), wetness (wet surfaces are stickier), chemistry (does the particle react with the surface), emissions (gases emitted by the surface).

It is easy to see from this wide range of processes that deposition is a very complicated process with many effects potentially driving the deposition of any given material. However, the two main factors that drive deposition are the friction velocity and particle size distribution[17]. Friction velocity takes into account both the wind speed and eddy turbulence, which are influential in determining interception and impaction,

[17] Erisman, J. W., Draaijers, G., Duyzer, J., Hofschreuder, P., Leeeuwen, N. V., Romer, F., Gallagher, M. (1997). "Particle Deposition to Forests - Summary of Results and Application". *Atmospheric Environment, 31*(3), 321-332.

and many of the effects of the surface[18]. Meanwhile particle size distribution determines the magnitude of the two other major processes (gravitational settling, and Brownian diffusion). Other sources[19,20] will note that deposition velocity is highly dependent on surface roughness, or roughness height, but these are inherent parameters in the friction velocity and thus are not independently significant.

Besides friction velocity and particle size distribution, density and shape of the particulate material are also considered as a secondary set of key parameters affecting deposition. However, the impact of these two properties is not universal across the size spectrum with small particles, those less than five μm, and large particles, those greater than 25 μm being insensitive to these values, whereas intermediate particles between these ranges are sensitive[21,22].

After the primary impact of friction velocity and particle size distribution, and the secondary impact of density and shape, the primary tertiary impact is relative humidity which can cause rapid growth or reduction in particle size[23]. However, at present it appears that the impact of relative humidity is as large as the uncertainty of the measured effect[24]. Other tertiary impacts include season of year and surface types[25] which influence leaf or foliar characteristics such as their size, presence, protuberances such as leaf hairs[26]. Leaf protuberances are known to affect the generation of and continuity of the laminar boundary layer adjacent to the leaf and thus influence impaction and interception of intermediate particles.

2.3. Section Summary

In the prior subsections the basics of deposition velocity and the various processes that govern deposition were covered. Many assumptions and limitations to the concept of deposition velocity were discussed, principle among them is the assumption that deposition is a steady-state horizontally and vertically homogenous process from the height at which air concentration is measured to the surface beneath. Thus, the height at which a measurement is taken is a critical parameter to accurately determining deposition velocity. Although many processes effect deposition velocity, the most significant factors are particle size distribution and friction velocity, with density and

[18] Donateo, A., & Contini, D. (2014). "Correlation of Dry Deposition Velocity and Fricition Velocity over Different Surfaces for PM2.5 and Particle Number Concentrations". *Advances in Meteorology.*
[19] Ibid.
[20] Jonsson, L., Karlsson, E., & Jonsson, P. (2008). "Aspects of Particulate Dry Deposition in the Urban Environment". *Journal of Hazardous Materials, 153*, 229-243.
[21] Ibid.
[22] Dare, R. A. (2015). *Sedimentation of Volcanic Ash in the HYSPLIT Dispersion Model - CAWCR Technical Report No. 079.* The Centre for Australian Weather and Climate Research. Melborne: The Centre for Australian Weather and Climate Research.
[23] Mohan, S. M. (2016). "An Overview of Particulate Dry Deposition: Measuring Methods, Deposition Velocity, and Controlling Factors". *International Journal of Environmental Science and Technology, 13*, 387-402
[24] Giorgi, F., (1988). "Dry Deposition Velocities of Atmospheric Aerosols as Inferred by Applying a Particle Dry Deposition Parameterization to a General Circulation Model". *Tellus, 40B*, 23-41
[25] Ibid.
[26] (Hicks, Saylor, & Baker, 2016)

shape factor being of lesser importance and primarily applicable only for particles in the five to 25 μm range.

Given the key factors from the previous paragraph, any good model for use by the FRMAC and Turbo FRMAC should be based on measurement made near the height at which FRMAC takes measurements (approximately one m). The model needs to be able to use particle size distribution information to calculate the friction velocity. Particle size density and shape factor is also needed, although defaults for all four parameters (friction velocity, particle size distribution, density, and shape factor) should be available.

Page Intentionally Blank

3. DEPOSITION MODELS

There are two major families of dry deposition models that are available in the literature. They are a family of models that are patterned after Sehmel[27] and those that are patterned after Slinn and Slinn[28]. Discussion of the "best of breed" models in these two families will follow later in their own respective subsections. But first a discussion of all models and their limitations will be covered.

However, before discussing model limitations, it needs to be pointed out that within these families there are generally five subcategories of models. The first category is devoid of particle size information and thus predicts a bulk deposition velocity over the whole size range of particles sizes[29,30]. The second kind is sized resolved, but applies to only a specific surface type (e.g. grassland) or a small subset of surface types[31,32,33,34,35,36,37,38,39,40]. The third category extends the second but generalizes it to a large number of surfaces[41,42,43].

A fourth category is a merger of the first and third/fourth categories that produced bulk deposition velocities but for a set of particles size ranges instead of specific particles or a single bulk velocity[44,45]. These models typically break particles into

---

[27] (Sehmel & Hodgson, A Model for Predicting Dry Deposition of Particles and Gases to Environment Surfaces - PNL-SA-6721, 1978)
[28] Slinn, S. A., & Slinn, W. G. (1980). "Predictions for Particle Deposition on Natural Waters". *Atmospheric Environment, 14*, 1013-1016.
[29] Wesely, M. L., Cook, D. R., Hart, R. L., & Speer, R. E. (1985). "Measurements and Parameterization of Particle Sulfur Deposition Over Grass". *Journal of Geophysical Research, 90*, 2131-2143.
[30] (Ruijgrok, Tieben, & Eisinga, 1997)
[31] Schack, C. J., Sotiris, E. P., & Friedlander, S. K. (1985). "A gneral correlation for Deposition of Suspended Particles from Turbulent Gases to Completely Rough Surfaces". *Atmospheric Environment, 19*, 983-1011.
[32] Ibrahim, M. L., Barrie, L. A., & Fanaki, F. (1983). "An Experimental and Theoretical Investigation of the Dry Deposition of Particles to snow, Pine Trees, and Artificial Collectors". *Atmospheric Environment, 17*, 781-788.
[33] Wiman, B. L., & Agren, G. I. (1985). "Aerosol Depletion and Deposition in Forests, A Model Analysis". *Atmospheric Environment, 19*, 335-362.
[34] Peters, K., & Eiden, R. (1992). "Modeling the Dry Deposition Velocity of Aerosol Particles to a Spruce Forest". *Atmospheric Environment, 26*, 2555-2564.
[35] Davidson, C. I., Miller, J. M., & Pleskow, M. A. (1982). "The Influence of Surface Structure on Predicted Particle Dry Deposition to Natural Grass Canopies". *Water Air Soil Pollution, 18*, 25-44.
[36] Legg, B. J., & Price, R. I. (1980). "The Contribution of Sedimentation to erosol Deposition to Vegatation with a Large Leaf Index". *Atmospheric Environment, 14*, 305-309.
[37] Bach, D. H. (1979). "Particulate Transport Within Plant Canopies (II)". *Atmospheric Environment, 13*, 1681-1687.
[38] Slinn, W. G. (1982). "Predictions of Particle Deposition to Vegetative Surfaces". *Atmospheric Environment, 16*, 1785-1794.
[39] (Slinn & Slinn, 1980)
[40] Williams, R. M. (1982). "A Model for the Dry Deposition of Particles to Natural Water Surfaces". *Atmospheric Environment, 16*, 1933-1938.
[4141] Giorgi, F. (1986). "A Particle Dry Deposition Parameterization Scheme for Use in Tracer Transport Models". *Journal of Geophysical Research, 91*, 9794 (Jonsson, Karlsson, & Jonsson, 2008)the-9804.
[42] Zhang, L. S., Gong, S., Padro, J., & Barrie, L. (2001). "A Size-Segregated Particle Dry Deposition Scheme for an Atmospheric Aerosol Module". *Atmospheric Environment, 35*, 549-560
[43] Nho-Kim, E. Y., Jackson, M. M., & Oskoie, V. H. (2001). "Development of an Atmospheric Particle Dry Deposition Model". *Aerosol Science and Technology, 38*, 627-636.
[44] (Feng, 2008)

ultrafine (less than 0.2 μm), coarse (greater than 2 μm), and intermediate particles[46]. There are two general reasons for this break down. The first is physical: ultrafines are controlled by Brownian diffusion, coarse by gravitational settling, and intermediates by inertial affects[47]. The second major reason is that field measurements show atmospheric peaks in these regions that are known as the nuclei, accumulation, and coarse modes[48].

The final and fifth category of deposition models are universal in the sense they can be applied to any particle size and any surface[49,50]. These models are the most general in their applicability as they are not tied to land use categories as the third type of model, and can use the surface roughness of any surface as an input.

In this report the focus will be on models in the third and fifth subcategories. The primary reason for this is the desire to make the NARAC model and Turbo FRMAC consistent with each other. The NARAC model is a size resolving model with access to land use category data, it thus can and does use models from the third category that are size resolving and generic to numerous surfaces. This need for and ability to handle generic surfaces eliminates the second subcategory of model.

The secondary reason is that the Turbo FRMAC and NARAC are simulating material that is very different from naturally occurring material in the environment, material for which both models have access to the expected particle size distribution. This difference between the expected particle size distributions and naturally occurring particle size distributions eliminates the fourth category of model which are fitted to particle size distributions of naturally occurring aerosols.

A tertiary reason is the need to make Turbo FRMAC and NARAC consistent with each other. A single bulk deposition velocity is what Turbo FRMAC already uses, and thus the first category is eliminated as it would simply replace the bulk deposition velocity with a new one, albeit based on updated assumptions and science.

Therefore, because of these three primary reasons, only models of subcategory three and five are valid options. Models in these categories for the two major model families will be discussed after the next section on model limitations that apply to all families and all subcategories of deposition models.

3.1. Model Limitations

The principle model limitation that must be understood amongst all the models is that each model produces predicted values that are an order of magnitude different than field derived data[51] for some range of the particle size spectrum. All models are

---

[45] Zhang, L., & He, Z. (2014). "Technical Note: An Emperical Algorithm Estimating Dry Deposition Velocity of Fine, Coarse, and Giant Particles". *Atmospheric Chemistry and Physics, 14*, 3729-3737.
[46] (Hicks, Saylor, & Baker, 2016)
[47] (Jonsson, Karlsson, & Jonsson, 2008)
[48] (Giorgi F. , 1988)
[49] (Sehmel & Hodgson, A Model for Predicting Dry Deposition of Particles and Gases to Environment Surfaces - PNL-SA-6721, 1978)
[50] Noll, K. E., & Fang, K. Y. (1989). "Development of a Dry Deposition Model For Atmospheric Coarse Particles". *Atmospheric Environment, 23*, 585-594.

generally at least an order of magnitude low in their prediction of deposition velocities in the 0.1 to 1 μm range[52,53], with some models two to three orders of magnitude lower in their predictions than observed in the field[54]. Between themselves, model agreement is typically better. However, models generally predict well for particles less than 0.1 μm and agree well in this range with field observations[55].

This limitation on prediction is not universal, but generally restricted to rough surfaces, with the agreement worsening with increasing surface roughness[56]. Although predictions between smooth surfaces and models is generally in good agreement, theoretical models suffer from large shortcomings and an inability to accurately predict deposition velocities for rough surfaces[57].

The limitation on prediction of particles in the intermediate regime (0.2 μm to 2 μm) is particularly important as the size spectrum of resuspended particles peaks near to this regime at roughly 3 μm[58]. Particle sizes in cities environments also peak around 2 μm[59]. Thus the range in which all models suffer is also the significant range for airborne particulate in the environment and the most likely particle size to be available for inhalation of resuspended material.

Another major limitation of all models is they treat the surface as a perfect sink[60]. In other words, particles deposit, but they never leave nor resuspend. Thus, all models neglect the impact of resuspension on the ground and air concentration. As already noted, resuspension reduces ground concentration and increases air concentration, thus this fundamental assumption and limitation of all deposition models will lead to underpredicting deposition velocities for particle sizes where resuspension is important. This assumption of a perfect sink occurs for all particles within one particle radius of the surface in both the Sehmel and Slinn and Slinn families[61].

Finally, predictive deposition models require that particles are diffusing from a constant flux of uniform concentration particles, that gravity only impacts settling velocity, and particles do not agglomerate on each other[62].

---

[51] McCready, D. I. (1986). "Wind Tunnel Modeling of Small Particle Deposition". *Aerosol Science and Technology, 5*, 301-312.
[52] (Feng, 2008)
[53] Petroff, A., Mailliat, A., Ameilh, M., & Anselmet, F. (2008). "Aerosol Dry Deposition on Vegetative Canopies, Part I: Review of Present Knowledge". *Atmospheric Environment, 42*, 3625-3653.
[54] Pellerin, G., Maro, D., Damay, P., Gehin, E., Connan, O., Laguionie, P., Charrier, X. (2017). "Aerosol Particle Dry Deposition Velocity Above Natual Surfaces: Quantification According to the Particles Diameter". *Journal of Aerosol Science, 114*, 107-117.
[55] Ibid.
[56] (Jonsson, Karlsson, & Jonsson, 2008)
[57] Ibid.
[58] Pryor, S. C., Larsen, S. E., Sorensen, L. L., & Barthelmie, R. J. (2008). "Particle Fluxes Above Forests: Observations, Methodological Considerations, and Method Comparisons". *Environmental Pollutions, 152*, 667-678.
[59] (Jonsson, Karlsson, & Jonsson, 2008)
[60] (Giorgi F. , 1988)
[61] (Hicks, Saylor, & Baker, 2016)
[62] (Sehmel, Particle Eddy Diffusivities and Deposition Velocities for Isothermal Flow and Smooth Surfaces, 1973)

Before moving on, a series of comments by Sehmel need to be discussed. The first is, "Once deposition from turbulent air flow can be predicted for isothermal conditions to smooth surfaces, the more complex problem of deposition to complex environmental surfaces may become amenable to analysis, generalization, and prediction."[63] As noted in this section, the prediction to smooth surfaces is generally quite good, thus the more complex problem of solving environmental deposition appears to be in reach.

However, Sehmel also notes "Predictive deposition velocity models must eventually consider both deposition within vegetative canopies as well as deposition penetration to the underlying surface. However, this penetration database in very limited and consequently penetration cannot be generalized in predictive models."[64] To this day the penetration databases are limited, and no generalization exists, and no model does a good job of considering deposition to the surface and penetration to the ground. It however is the case that models of the Slinn and Slinn family, particularly Petroff and Zhang attempt to do so, while models of the Sehmel family make no such attempt. However, given the limitation of the penetration database it will be seen that there is not much difference between these models.

To conclude this section, Sehmel states, "The real practical problems now are in determining methods for predicting particle deposition to environmental surfaces in which factors such as surface roughness, particle agglomeration, impaction, interception, temperature gradients, moisture gradients, and electrical gradients are important in the deposition process."[65] None of the available models treat most of these effects except for surface roughness which is a direct parameter in Sehmel family models and more indirect in the Slinn and Slinn models. The Slinn and Slinn models generally have greater treatment for interception and impaction than do the Sehmel family models, although the difference will be seen to be minor. Thus, all models are inherently limited when compared to the field observations in that they do not consider agglomeration, important environmental gradients, and other effects that are influential on the microscale.

3.2. Sehmel Family

The Sehmel family of models consist of three principle models. They are the last of a series of progressively elaborated models produced by Sehmel himself[66], an update to his model produced by Noll and Fang[67], a furtherance of Noll and Fang's model by Feng[68]. This section is broken down into a description of the Sehmel model, a

[63] Ibid.
[64] (Sehmel & Hodgson, A Model for Predicting Dry Deposition of Particles and Gases to Environment Surfaces - PNL-SA-6721, 1978)
[65] (Sehmel, Particle Eddy Diffusivities and Deposition Velocities for Isothermal Flow and Smooth Surfaces, 1973)
[66] (Sehmel & Hodgson, A Model for Predicting Dry Deposition of Particles and Gases to Environment Surfaces - PNL-SA-6721, 1978)
[67] (Noll & Fang, Development of a Dry Deposition Model For Atmospheric Coarse Particles, 1989)
[68] Feng, J. (2008). "A Size-Resolved Model and a Four-Mode Parameterization of Dry Deposition of Atmospheric

description of the Noll and Fang model, a description of the Feng model, and a comparison between the three models.

3.2.1. Description of Sehmel

Prior to the first of the Sehmel series of models[69] deposition velocity was assumed to be caused by the free flight of a particle to a surface. At some point away from the surface eddy diffusion was assumed to instantly stop. This model of deposition required defining some arbitrary distance at which eddy diffusion stopped and the determination of an arbitrary velocity towards the surface from the point at which eddy diffusion stopped. This velocity was known as the free flight velocity.

None of the research prior to this had derived distances or velocities that matched laboratory data well. The major advancement of Sehmel was to devise an effective diffusion coefficient that incorporated the effects of eddy diffusion, inertial effects, and shear forces. From this development of effective eddy diffusion, Sehmel then devised a model that included Brownian diffusion (ultrafine particles), effective eddy diffusion (intermediate particles), and terminal settling velocity (coarse particles). The detailed description of his model that follows is derived from (Sehmel & Hodgson, A Model for Predicting Dry Deposition of Particles and Gases to Environment Surfaces - PNL-SA-6721, 1978), but other details and the progression of development can be found in Sehmel's earlier reports[70,71,72].

The deposition flux of a contaminant can be derived from the following formula.

* MERGEFORMAT [3.1]

$$N = -(\varepsilon + D)\frac{dC}{dz} - v_t C$$

where

- N is the deposition flux
- ε is the particle eddy diffusivity
- D is Brownian diffusivity
- C is the concentration of the contaminant
- vt is the particles settling velocity
- z is the height above a surface

Aerosols". *Journal of Geophysical Research, 113*, D12201.

[69] Sehmel, G. A. (1970). "Particle Deposition from Turbulent Air Flow". *Journal of Geophysical Research, 75*(9), 1766-1781.

[70] (Sehmel, Particle Deposition from Turbulent Air Flow, 1970)

[71] (Sehmel, Particle Diffusivities and Deposition Velocities over a Horizontal Smooth Surface, 1971)

[72] (Sehmel, Particle Eddy Diffusivities and Deposition Velocities for Isothermal Flow and Smooth Surfaces, 1973)

Deposition velocity is then predicted from a dimensionless integral form of * MERGEFORMAT [3.1]

* MERGEFORMAT [3.2]

$$\int_{C_z}^{0} \frac{u_* dC}{N + v_t C} = \int_{z^+ = C_z}^{r^+} \frac{dz^+}{\frac{\varepsilon}{\nu} + \frac{D}{\nu}} = Int$$

where

- u_* is the friction velocity
- z^+ is the dimensionless distance above the surface (defined further below)
- ν is the kinematic viscosity of air
- Int is a shorthand notation used in Sehmel papers for the right-hand size of * MERGEFORMAT [3.2]
- C_z is the contaminants concentration at a reference height z
- r^+ is the distance from the surface of one dimensionless particle radius

The integral Int is then subdivided in Sehmel's papers as follows

* MERGEFORMAT [3.3]

$$Int = \int_{z^+ = C_z}^{z^+_{1-2}} \frac{dz^+}{\frac{\varepsilon}{\nu} + \frac{D}{\nu}} + \int_{z^+_{1-2}}^{z^+_{2-3}} \frac{dz^+}{\frac{\varepsilon}{\nu} + \frac{D}{\nu}} + Int_3$$

where

- Int_3 is

* MERGEFORMAT [3.4]

$$Int_3 = -e^{\left(-378.051+16.498*\ln(Sc)+\ln(t^+)*\left(-11.818-0.2863*\ln(t^+)+0.3226*\ln\left(\frac{D}{z_o u_*}\right)\right)-12.804*\ln(d)\right)}$$

where

- Sc is the Schmidt number
- t^+ is the dimensionless relaxation time
- z_o is the roughness length of the surface
- d is the particle diameter

The three subinterval variables in the Int term will correspond to terms in the Slinn and Slinn models that are referred to as resistances. These three terms represent the

resistance due to atmospheric motion or aerodynamic resistance, the resistance due to quasi-laminar flow about a surface, and the resistance to interception by the surface. They will be seen to correspond to the r_a, r_b, and r_c terms of the Slinn and Slinn family of models.

The eddy term ε is not defined in the Sehmel model directly, and instead is defined by a fit to experimental wind tunnel data[73]. The term that is actually defined in the normalized effective eddy diffusivity ε / ν which is defined by equations * MERGEFORMAT [3.5], * MERGEFORMAT [3.7], and * MERGEFORMAT [3.8]. The first of these equation is:

* MERGEFORMAT [3.5]
$$\frac{\varepsilon}{\nu} = \psi \left(z^+\right)^{2.6} \left(t^+\right)^{1.2}$$

where

- ψ a fit multiplier
- all other terms are as before

Ψ is defined by the equation:

* MERGEFORMAT [3.6]
$$\psi = 0.531 e^{-0.033 u^*}$$

The value of ε / ν is bound by the following equations and is maximal at a value of 140 (ε / ν is dimensionless). The upper bound of ε / ν is:

* MERGEFORMAT [3.7]
$$\frac{\varepsilon}{\nu} = 1.1 z^+$$

The lower bound of ε / ν is:

* MERGEFORMAT [3.8]
$$\frac{\varepsilon}{\nu} = 0.002 * \left(\frac{z^+}{10}\right)^3$$

Brownian diffusion D is defined as:

* MERGEFORMAT [3.9]
$$D = \left(\frac{kT}{6\pi\mu r}\right)\left(1 + \frac{1e-4}{pr}\left(6.32 + 2.01 e^{-2190\, pr}\right)\right)$$

where

- k is Boltzmann's constant

[73] (Sehmel, Particle Eddy Diffusivities and Deposition Velocities for Isothermal Flow and Smooth Surfaces, 1973)

- T is the temperature.
- μ is the air absolute viscosity
- r is the particle radius
- p is the pressure

Terminal setting velocity v_t is defined by

* MERGEFORMAT [3.10]

$$v_t = \frac{\rho_p g d^2}{18\mu}$$

where

- ρ_p is the density of the particle
- g is the gravitational constant

The friction velocity u_* is defined by

* MERGEFORMAT [3.11]

$$u_* = \frac{ku(z)}{\ln\left(\frac{z+z_o}{z_o}\right)}$$

where

- k is the Von Karmen constant (0.4)
- z_o is the roughness length of a surface element
- u(z) is the wind speed at height z

The dimensionless height z^+ is defined by

* MERGEFORMAT [3.12]

$$z^+ = \frac{zu_*}{v}$$

The dimensionless particle radius r^+ uses * MERGEFORMAT [3.12] with r replacing z.

The kinematic viscosity coefficient is defined by

* MERGEFORMAT [3.13]

$$v = \frac{\mu}{\rho_a}$$

where

- ρ_a is the density of air which is calculated from

* MERGEFORMAT [3.14]
$$\rho = \frac{P}{RT}$$

where

- R is the gas constant for dry air

The Schmidt number (Sc) is defined by

* MERGEFORMAT [3.15]
$$Sc = \frac{\nu}{D}$$

The dimensionless relaxation time is defined by

* MERGEFORMAT [3.16]
$$t^+ = \left(\frac{\rho_p d^2}{18\mu}\right)\left(\frac{u_*^2}{\nu}\right)$$

The absolute (dynamic) viscosity of air is defined by

* MERGEFORMAT [3.17]
$$\mu = \mu_o \left(\frac{T_o + C}{T + C}\right)\left(\frac{T}{T_o}\right)^{\frac{3}{2}}$$

where

- μ_o is the reference viscosity at reference temperatures (18.27 μPa * s for dry air)
- T_o is the reference temperatures (291.15 K for dry air)
- C is a coefficient of fit (120 K for dry air)

With all terms defined, equation * MERGEFORMAT [3.2] can be integrated to derive

* MERGEFORMAT [3.18]
$$N = \frac{\nu_t C_z \alpha}{1 - \alpha}$$

where α is defined by

* MERGEFORMAT [3.19]
$$\alpha = e^{\left(\frac{-\nu_t Int}{u_*}\right)}$$

Recalling that deposition velocity is deposition flux over air concentration yields

* MERGEFORMAT [3.20]

$$V_d = \frac{-N}{C_z}$$

or

* MERGEFORMAT [3.21]

$$V_d = \frac{v_t}{1 - \frac{1}{\alpha}}$$

which now fully defines the deposition velocity model of Sehmel.

The deposition velocity model of Sehmel has several unique and important characteristics. First, it is applicable to any kind of surface for which a roughness length is defined. Second, it implicitly includes the particle size, density, and friction velocity. Thus, Sehmel includes all the essential and critical parameters for determining deposition velocity as noted in Section 2.2. Through the particle size term and an update to the terminal settling velocity formulation secondary effects such as particle shape can be included.

Thirdly, it is the only deposition model whose data fits are based on actually known boundary and initial conditions since the data used to derive the fits come from wind tunnel data. All other models use field observations for with these conditions are not known and are assumed. Fourthly, the Sehmel model is derived using fits, observations, and data for heights of a couple cm[74,75,76] or 1 m[77], all of which are much closer to the height at which FRMAC monitoring and sampling teams would make observations. Other models use data derived from 18 m to 30 m or higher values. This is important to remember for future sections, and to pull forward the knowledge that observation of air concentration at higher elevations by definition require higher deposition velocities.

3.2.2. Description of Noel

The model of Noel and Fang[78] uses the model of Sehmel as its base formulation and was primarily developed because the model of Sehmel does not account for inertial deposition of particles greater than approximately 30 μm[79]. Noel used field measurement work[80] to update the fits to the Sehmel model and produce a new model

[74] (Sehmel, Particle Deposition from Turbulent Air Flow, 1970)
[75] (Sehmel, Particle Diffusivities and Deposition Velocities over a Horizontal Smooth Surface, 1971)
[76] (Sehmel, Particle Eddy Diffusivities and Deposition Velocities for Isothermal Flow and Smooth Surfaces, 1973)
[77] (Sehmel & Hodgson, A Model for Predicting Dry Deposition of Particles and Gases to Environment Surfaces - PNL-SA-6721, 1978)
[78] (Noll & Fang, Development of a Dry Deposition Model For Atmospheric Coarse Particles, 1989)
[79] Ibid.
[80] Lin, J. J., Noll, K. E., & Holsen, T. M. (1994). "Dry Deposition Velocities as a Function of Particle Size in the

described in Noel, Jackson, and Oskouie[81] which is known as the Noel or Noel and Fang model.

The updated formulations follow and only those aspects of the equations that differ from Sehmel are directly described.

Noel defines deposition velocity as follows

* MERGEFORMAT [3.22]
$$V_d = V_{st} + V_{di} + V_{dd}$$

where

- V_{st} is the Stokes Law terminal gravitational settling velocity.
- V_{di} is the particle's deposition velocity due to inertial effects (impaction and interception).
- V_{dd} is the particle's deposition velocity due to Brownian motion

The definition of V_{st} is nearly identical to Sehmel but adds the Cunningham Slip correction. V_{st} is thus defined as

* MERGEFORMAT [3.23]
$$V_{st} = \frac{C_c p_p g d_p^2}{18\mu}$$

where

- C_c is the Cunningham slip coefficient defined as

* MERGEFORMAT [3.24]
$$C_c = 1 + \frac{2\lambda}{d_p}\left(1.257 + k * e^{\frac{-1.1 d_p}{2\lambda}}\right)$$

where

- λ is the mean free path of an air molecule defined by

* MERGEFORMAT [3.25]
$$\lambda = \frac{2\mu}{p\sqrt{\left(\frac{8M}{\pi RT}\right)}}$$

where

- M is the molecular weight of dry air

The inertial velocity V_{di} is defined by the equation

Ambient Atmosphere". *Aerosol Science and Technology, 1994*, 239-252.

[81] Noll, K. E., Jackson, M. M., & Oskouie, A. K. (2001)." Development of an Atmospheric Particle Dry Deposition Model". *Aeorsol Science and Technology, 35*, 627-636.

* MERGEFORMAT [3.26] $$V_{di} = 0.024175e^{-0.5\left(\frac{\mathrm{Re}-40300}{3833.25}\right)^2} + 1.4911534e^{-0.5\left(\frac{\ln\left(\frac{t^+}{18}\right)}{1.7}\right)^2}$$

where

- Re is the Reynolds number of the flow which is defined by

* MERGEFORMAT [3.27] $$\mathrm{Re} = \frac{\rho u D_p}{\mu}$$

Noel uses an updated form for Brownian Diffusion (D) which is

* MERGEFORMAT [3.28] $$D = \frac{kTC_c}{3\pi\mu d_p}$$

The formula for the Brownian velocity V_{dd} is then

* MERGEFORMAT [3.29] $$V_{dd} = 0.084Sc^{-2/3}$$

This completes the definition of the Noel and Fang model.

3.2.3. Feng

The model of Feng[82] is an extension to the Noel and Fang model. The model was devised when it was noted that the discrepancy between model data and measurements suggested a missing mechanism for deposition. The mechanism proposed by Feng is the so called burst effect of eddy turbulence, or as defined previously, turbophoresis. The burst effect is caused by the tendency of particles to migrate to areas of lower turbulence. Since the normal assumption of uniformity of turbulence is not true in practice most models ignore the influence of this effect. Observations have shown that a particle move towards the surface (region of no turbulence) through high speed penetrations or bursts (the burst effect), while movement away from the surface is slower[83] or restricted.

This effect is important because it is most influential to particles in the critical regime of intermediate particles where all models typically underestimate deposition velocity by an order of magnitude or more. Thus, a mechanism that burst the material to the surface and enhances impaction and interception is potentially critical to accurately calculating deposition velocity.

Feng's model comes in both a generalized particle size specific model and a four-bin model. Description of each follows.

[82] (Feng, 2008)
[83] Ibid.

3.2.3.1. Arbitrary Particle Size

The formulation of the arbitrary particle size model follows that of Noel and the equation for deposition velocity is

* MERGEFORMAT [3.30]
$$V_d = V_t + u_* \left(Sc^{-0.6} + 0.0226 e^{-0.5\left(\frac{\left(\mathrm{Re}^* - 40300\right)}{15330}\right)^2} + 0.8947 e^{-0.5\left(\frac{\left(t^+ - 18\right)}{1.7}\right)^2} \right)$$

where

- Re^* is the roughness Reynolds number defined by the equation

* MERGEFORMAT [3.31]
$$\mathrm{Re}^* = \frac{u_* z_o}{\mu}$$

The roughness Reynolds number accounts for the fact that atmospheric turbulence is more characterized by the wind field and roughness of the surface whereas the Reynolds number accounts more for the turbulence around the particle. Hence, to properly account for turbophoresis it is appropriate to consider the turbulence of the atmosphere, not the turbulence around the particle.

This fully defines Feng's particle size specific model. Feng's model has all the positive attributes of Noel's model, but now includes the influence turbophoresis. As will be seen in the comparison sections that follow, this is a critical edition that Feng made which has gone generally unrecognized by the community.

3.2.3.2. Bin Model

Feng's bin model divides the particle spectrum up into four particle sizes. Those bins are described in Table 2. For each bin the deposition velocity is determined as follows

* MERGEFORMAT [3.32]

$$V_{di} = V_{si} + \frac{1}{R_a + \frac{1}{\left(V_{d1} + a_i u_*^{b_i}\right)}}$$

where

- V_{di} is the bin averaged deposition velocity.
- V_{si} is the bin averaged settling velocity.
- a_i and b_i are coefficients of fit that are show in Figure 2.
- V_{d1} is the contribution due to turbophoresis and eddy diffusion that is not particle size specific and is defined by the equation

* MERGEFORMAT [3.33]

$$V_{d1} = u_* 0.226 e^{-0.5\left(\frac{\mathrm{Re}-40300}{15330}\right)^2}$$

Table 1: Particle size bin's used in Feng's model.

Bin	Minimum Particle Size (µm)	Maximum Particle Size (µm)
Nucleation Mode	0.001 (1 nm)	.1
Accumulation Mode (Turbophoresis dominated)	.1	2.5
Coarse Mode	2.5	10
Giant Mode	10	100

Table 1. Coefficients of Power Law Regression $V_{d2} = au_*^b$ for the Whole Aerosol Size Spectrum and for Four Modes

	Bulk Parameterization for the Whole Size Range		Mode 1		Mode 2		Mode 3		Mode 4	
	a	*b*	*a*	*b*	*a*	*b*	*a*	*b*	*a*	*b*
Urban	0.5256	1.4449	0.0048	1.0000	0.0315	2.7925	1.2891	2.6878	1.0338	1.2644
Remote Conti.	0.8191	1.4467	0.0037	1.0000	0.0120	2.2413	1.3977	2.5838	1.0707	1.3247
Desert	0.9138	1.0405	0.0042	1.0000	0.2928	3.8581	1.3970	2.5580	0.9155	1.0364
Polar	0.7537	1.3234	0.0032	1.0000	0.1201	3.4407	1.1838	2.8033	1.0096	1.2069
Marine	0.8132	1.8476	0.0043	1.0000	0.1337	3.5456	1.2834	2.7157	1.1595	1.4863
Rural	0.6886	1.6545	0.0045	1.0000	0.0925	3.2920	1.2654	2.7227	1.0891	1.3654
Free Trop.	0.9454	1.6994	0.0039	1.0000	0.2859	3.8558	1.3072	2.6840	1.1242	1.4240

Figure 2: Reproduction of Table 1 from (Feng, 2008).

V_{si} is defined by the equation

* MERGEFORMAT [3.34]

$$V_{si} = \int_{d_{\min}}^{d_{\max}} F(d_p) V_s(d_p) dd_p$$

where

- F is the fraction of the particle size distribution represented by particle size of diameter d_p
- d_{min} is the minimum particle size in the particle size distribution
- d_{max} is the maximum particle size in the distribution

The value for R_a is defined as

* MERGEFORMAT [3.35]

$$R_a = \frac{1}{ku_*} \begin{pmatrix} \ln\left(\frac{z}{z_o}\right) + 4.7(\zeta - \zeta_o) \\ \ln\left(\frac{z}{z_o}\right) \\ \ln\left(\frac{z}{z_o}\right) + \ln\left(\frac{(\eta_o^2+1)(\eta_o+1)^2}{(\eta^2+1)(\eta+1)^2}\right) + 2\left(\tan^{-1}(\eta) - \tan^{-1}(\eta_o)\right) \end{pmatrix} \begin{pmatrix} Stable \\ Neutral \\ Unstable \end{pmatrix}$$

where

- stable, neutral, and unstable refer to the atmospheric lapse rate dT/dz being greater than zero, zero, and less than zero respectively

η is defined by the equation

* MERGEFORMAT [3.36]

$$\eta = (1 - 15\zeta)^{\frac{1}{4}}$$

where ζ is defined by the equation nullifying

* MERGEFORMAT [3.37]

$$\zeta = \frac{z}{L_m}$$

where

- L_m is the Monin-Obukhov length defined as

* MERGEFORMAT [3.38]

$$L_m = \frac{\rho_a c_p T_o u_*^3}{kgq_o}$$

where

- ρ_a is the density of dry air
- c_p is the specific heat at constant pressure for dry air
- T_o is the surface temperature
- q_o is the vertical flux of sensible heat at the ground which is defined as

* MERGEFORMAT [3.39]

$$q_o = \frac{\int_0^z kq(z)dz}{\int_0^z \ln(z) - \psi(z/L)dz}$$

Note that to solve for R_a a value for L_m is required, which requires a value for q_o which requires a value for L_m. The solution to which requires an initial guess for a value of L and an iterative technique until convergence occurs.

The definition of η_o is the same as η but with ζ replaced with ζ_o. ζ_o is defined as ζ but with z replaced by z_o.

This now fully defines the bin model of Feng. It can easily be determined that the bin model of Feng is substantially more complicated in computation than the arbitrary particle size model. It further introduces the need for iteratively solving for the heat flux and Monin-Obukhov length. However, it is advantageous for models that do not track particular particle sizes but mass within each bin when the definition of V_{si} is coupled with presumed particle size distributions which is done in (Feng, 2008) but not described here.

A principle advantage of both of Feng's models, as will be described later, is he followed upon Sehmel, Noel, Slinn, and Zhang, to incorporate the best of all. As will be seen, this enable his model to overcome many of the shortcomings of these models, producing both a simple, and an accurate model.

3.2.4. Comparison

As already noted both Sehmel, Noel and Fang, and Feng are universal models that are applicable to any surface type so long as a roughness length has been defined for the surface. For any surface the roughness length is approximate the average height of the obstructions divided by 30[84], and thus readily determinable for any situation.

In addition, these models capture all critical aspects of calculating a deposition velocity because they consider friction velocity and particle size (radius and diameter)

[84] (Seinfeld & Pandis, 2012)

parameters. But how do the these models compare with each other and what are the pros and cons between the three of them?

Several studies have been performed that analyzed field data and compared their results to these models. The first was done by Noll[85] in which Noll's model captured the underprediction of deposition velocity for large (greater than 30 μm) particles better than Sehmel's. However, it is not surprising that Noll's model[86] captured Noll's data[87] better than Sehmel's model which did not have the advantage of using this additional dataset for curve fitting. Lin[88] hypothesized that the better agreement is due to Noll's model capturing the impartation of momentum from atmospheric particles to particles in the inertial subrange that is not captured by Sehmel. This is possible through Noel's introduction of the Reynolds number and ability of this number to indicate the magnitude of inertial motion. Lin's work also concluded that although several models all fit the data in the paper well, Sehmel was the best fit to overall mass flux surpassing the initial Noel and Fang, and Slinn family models.

A second report by Fang[89] which performed an independent study of deposition velocity using field observations in Taiwan came to the conclusion that Noll and Fang showed slightly better agreement to measured results than did the Sehmel model.

A third, and most recent study by Mohen[90] which review global deposition velocity data concluded that Noel and Fang predicts better than Sehmel for particles in the inertial range but that Sehmel performed better in mixed urban environments.

The general conclusion of available results is that the updated version of the Noel and Fang model surpasses Sehmel in predictive capability, although for particles smaller than five μm Sehmel is still likely the better model. However, as will be seen in the final comparison of all models, the model of Feng brings in the best of both the Slinn and Slinn and Sehmel/Noel worlds, and through the introduction of turbophoresis, produces the only model capable of predicting deposition velocities on the order of one cm / s for the critical accumulation model particles.

Besides being the better model from a prediction standpoint, Noel and Fang and Feng have one other great advantage over Sehmel. They do not require solving the complicated INT integral that is part of the Sehmel model. They further use readily available flow parameters through the Reynolds or roughness Reynolds number to incorporate the influence of eddy diffusion and turbophoresis.

3.3. Slinn Family

The Slinn family of models are a series of models that are described as being resistive in nature[91] in that deposition velocity is calculated in a way similar to the current flow

[85] (Noll, Jackson, & Oskouie, Development of an Atmospheric Particle Dry Deposition Model, 2001)
[86] Ibid.
[87] (Lin, Noll, & Holsen, 1994)
[88] Ibid.
[89] Fang, G. C., Wu, Y. S., Chang, C. N., Chang, K. F., & Yang, D. G. (1999). "Modeling Dry Deposition of Total Particulate Mass In Trafficked and Rural Sites of Central Taiwan". *Environment International, 5*, 625-633.
[90] (Mohan, 2016)
[91] (Petroff, Mailliat, Ameilh, & Anselmet, 2008)

through a series of resistors in series. In these models the resistors are regions of the atmosphere each of which are given a resistance that is used to calculate the velocity (current) through them. These models ignore settling due to gravity in each of the resistive terms, adding gravity in after the fact through a settling velocity term[92].

Compared to the Sehmel family of models there is a lot of criticism of the resistive models. Several recent papers[93,94,95] have drawn attention to the inadequacies of resistive models and a later section of this paper will call great attention to the deficiencies and susceptibility of the data upon which they rest. Furthermore, it has been noted that resistive models are inapplicable to aerodynamically very rough surfaces[96] such as urban environments. Another criticism of resistive models is that the only way to get them to agree with data is if the parameters within the models are pushed to applicable limits[97], suggesting that the underlying principles are in error. A final limitation is that these models are designed for regional scale modeling and use roughness lengths applicable to large regions[98] such as a forest or pastureland.

However, all is not lost with the Slinn family of models. Unlike the Sehmel family of models, they provide terms (in some cases) for including the secondary effects of vegetative surface area, orientation, phoretic effects, and other secondary and tertiary effects. These effects were noted at the start of this document as other potentially important parameters[99] in the calculation of deposition velocity. These terms, available in the Slinn family of models have no corollaries in the Sehmel family.

These key limitations and advantages being noted it is important to note that there are several major subsets of models in this category. Those that apply to only a specific particle size range, or specific surface are hereby eliminated and will not be discussed. Only those models that are applicable to all surfaces and all particle sizes are discussed in depth. Major models to discuss are the progenitor model of Slinn and Slinn; the most widely used and accepted model of Zhang, which comes in both a particle size binned and specific particle size distribution version; and the most recent and detailed update of Zhang produced by Zhang and Petroff.

After discussing each of these models, issues surrounding the data used to fit these models will follow. Finally, a comparison between the models will be discussed. In

---

[92] Ibid.
[93] (Hicks, Saylor, & Baker, 2016)
[94] Seinfeld, J. H., & Pandis, S. N. (2012). *Atmospheric Chemistry and Physics: From Air Polution to Climate Change.* New York: John Wiley.
[95] Venkatram, A., & Pleim, J. (1999). The Electrical Analogy does not Apply to Modeling Dry Deposition of Particles. *Atmospheric Environment, 33*, 3075-3076.
[96] (Mohan, 2016)
[97] (Pryor, Larsen, Sorensen, & Barthelmie, Particle Fluxes Above Forests: Observations, Methodological Considerations, and Method Comparisons, 2008)
[98] Gallagher, M. W., Nemitz, E., Dorsey, J. R., Fowler, D., Sutton, M. A., Flynn, M., & Duyzer, J. (2002). "Measurement and Parameterizations of Small Aerosol Deposition Velocities to Grassland, Arable Crops, and Forests: Influence of Surface Roughness Lenght on Deposition". *Journal of Geophysical Research, 107*(12), 8-1 to 8-10.
[99] (Hicks, Saylor, & Baker, 2016)

the discussions that follow, unless terms differ in definition from those of the Sehmel family of models, they will not be redefined.

3.3.1. Description of Slinn

In the Slinn family of models the calculation of deposition velocity is formulated as follows

* MERGEFORMAT [3.40]

$$V_d = V_s + \frac{1.0}{R_a + R_b}$$

where

- R_a is the aerodynamic resistance of the general atmosphere (eddy diffusion term of Sehmel)
- R_b is the quasi-laminar and surface resistance, sometime broken into R_b and R_c depending on the author and publication

The aerodynamic resistance is defined as

* MERGEFORMAT [3.41]

$$R_a = \frac{1.0}{C_d u}$$

The quasi-laminar and surface resistance is defined as

* MERGEFORMAT [3.42]

$$R_b = \frac{1.0}{u_* \left(E_{br} + E_{im} + E_{in}\right)}$$

where

- E_{br} is the surface collection efficiency due to Brownian motion
- E_{im} is the surface collection efficiency due to impaction
- E_{in} is the surface collection efficiency due to interception

All terms contain parameters that are fit to a specific kind of surface and thus they do not have the general applicability of the Sehmel family of models. Thus, a major limitation of all Slinn family models is the range of surfaces to which they have been fitted.

E_{br} is defined as

* MERGEFORMAT [3.43]

$$E_{br} = Sc^{-\gamma}$$

where

- γ is 0.5 for water and 2/3 for vegetation.

E_{im} is defined as

* MERGEFORMAT [3.44]

$$E_{im} = \left(\frac{St}{St + \alpha} \right)^{\beta}$$

where

- α is a coefficient of fit (0.8 for Slinn)
- β is a coefficient of fit (2.0 for Slinn)
- and St is the Stokes number defined as

* MERGEFORMAT [3.45]

$$St = \frac{C_c u \rho_p d_p^2}{18 \mu L}$$

where

- L is the characteristic diameter of the obstacle (vegetation in this case).

E_{in} is defined as

* MERGEFORMAT [3.46]

$$E_{in} = \left(\frac{C_v}{C_d} \right) \left(F \left(\frac{r}{r + r_{veg}} \right) + (1 - F) \left(\frac{r}{r + R_{veg}} \right) \right)$$

where

- C_v/C_d is the ratio (0.3) of the viscous drag to the total drag
- F is the fraction of total interception (1%) by the impactor (e.g. leaf)
- r_{veg} is the characteristic radius of vegetative hairs (10 μm)
- R_{veg} is the characteristic radius of large interceptors (1 mm for forests, 0.5 mm for other vegetation. R_{veg} is used as L in * MERGEFORMAT [3.45])

This completes the definition of the Slinn model.

It is easy to note that the Slinn model is generally applicable to any particle size, and to any surface. Like the Sehmel family of models through gravitational settling and the u_* term the primary factors of particle size and surface roughness are included in the models. However, the model presents more problems than the Sehmel family of models. First, to apply to any particular surface a number of essentially impossible parameters to ascertain are needed. This include the radius of leaf hairs, the radius of larger vegetative impactors, the fraction of interception caused by vegetative hairs versus larger impactors and the characteristic length of the obstacle of impaction. All of these parameters are very surface specific and require the assumption of universality of the surface vegetation. There can be no mixing of plant species.

In addition to these parameter, several other parameters of fit are required for the Slinn model. They include the α, β,and γ coefficients which are themselves surface, and

surface state-specific. Trees blowing in the wind or water surface covered by waves do not have the same coefficients as trees that are stationary or water that is calm.

3.3.2. Description of Zhang

The model of Zhang is the most commonly implemented and heavily used operational model[100] of any of the deposition models currently available. It is optimized for and used extensively by operational weather forecast models and thus is designed to be used on the scale of tens to hundreds of km grid cell spacing. The model comes in two primary forms. A version meant to be applied to an arbitrary particle size distribution[101] and a form designed for three main particle size bins[102] that have been noted in Section 3. These two models will be described in more detail in their own subsection.

3.3.2.1. Arbitrary Particle Size Model

In the model of Zhang R_a is defined as

* MERGEFORMAT [3.47]

$$R_a = \frac{\ln\left(\frac{z}{z_o}\right) - \psi_h}{k u_*}$$

where

- ψ_h is the stability function defined as[103]

* MERGEFORMAT [3.48]

$$\psi_h = 2\ln\left(\frac{1+\left(1-16\frac{z}{L_m}\right)^{\frac{1}{2}}}{2}\right)$$

The definition of R_b is

* MERGEFORMAT [3.49]

$$R_b = \frac{1.0}{\varepsilon_o u_* \left(E_{br} + E_{in} + E_{im}\right) R_1}$$

where

- ε_o is an empirical constant of value 3
- R_1 is a correction factor for the number of particles that stick to a surface upon impaction defined by the equation

---

[100] Petroff, A., & Zhang, L. (2010). "Development and Validation of a Size-Resolved Particle Dry Deposition Scheme For Applications in Aerosol Transport Models". *Geoscience Model Development Discussions, 3*, 1317-1357

[101] (Zhang, Gong, Padro, & Barrie, 2001)

[102] (Zhang & He, 2014)

[103] Paulson, C. A. (1970). "The Mathematical Representation of Wind Speed and Temperature Profiles in the Unstable Atmospheric Surface Layer". *Journal of Applied Meteorology, 9*, 857-861.

* MERGEFORMAT [3.50]

$$R_1 = e^{-St^{\frac{1}{2}}}$$

The definition of E_{br} and E_{im} are unchanged, but the α and γ coefficients are unique for each land use category available in the model. The β coefficient retains a value of 0.2.

The definition of E_{in} changes to be

* MERGEFORMAT [3.51]

$$E_{in} = \frac{1}{2}\left(\frac{d_p}{A_{veg}}\right)^2$$

In all the equations above the dry radius or diameter are replaced by the wet radius or diameter which is calculated using the function

* MERGEFORMAT [3.52]

$$r_w = \left(\frac{C_1 r_d^{C_2}}{C_3 r_d^{C_4} - \ln(RH)} + r_d^3\right)$$

where

- RH is the relative humidity
- r_d is the dry radius (or diameter)
- C_x coefficients are coefficients of fit provided in Figure 3

Table 1
Constants for Eq. (10)

Aerosol model	C_1	C_2	C_3	C_4
Sea salt	0.7674	3.079	2.573×10^{-11}	− 1.424
Urbal	0.3926	3.101	4.190×10^{-11}	− 1.404
Rural	0.2789	3.115	5.415×10^{-11}	− 1.399
$(NH_4)_2SO_4$	0.4809	3.082	3.110×10^{-11}	− 1.428

Figure 3: Reproduction of Table 1 from (Zhang, Gong, Padro, & Barrie, 2001).

Figure 4 is a reproduction of Table 2 from (Zhang, Gong, Padro, & Barrie, 2001) which shows the landuse categories while Figure 5 is a reproduction of Table 3 which contains the values of all other coefficients by landuse type.

Table 2
Land use categories (LUC) and seasonal categories (SC) used in Canadian Aerosol Module

Category	Description
Land use categories (LUC)	
1	Evergreen–needleleaf trees
2	Evergreen broadleaf trees
3	Deciduous needleleaf trees
4	Deciduous broadleaf trees
5	Mixed broadleleaf and needleaf trees
6	Grass
7	Crops, mixed farming
8	Desert
9	Tundra
10	Shrubs and interrupted woodlands
11	Wet land with plants
12	Ice cap and glacier
13	Inland water
14	Ocean
15	Urban
Seasonal categories (SC)	
1	Midsummer with lush vegetation.
2	Autumn with cropland that has not been harvested.
3	Late autumn after frost, no snow.
4	Winter, snow on ground and subfreezing.
5	Transitional spring with partially green short annuals.

Figure 4: Reproduction of Table 2 from (Zhang, Gong, Padro, & Barrie, 2001).

Table 3
Parameters for 12 land use categories (LUC) and five seasonal categories (SC)*

LUC		1	2	3	4	5	6	7	8	9	10	11	12	13	14	15
	SC 1	0.8	2.65	0.85	1.05	1.15	0.1	0.1	0.04	0.03	0.1	0.03	0.01	$f(u)$	$f(u)$	1.0
	SC 2	0.9	2.65	0.85	1.05	1.15	0.1	0.1	0.04	0.03	0.1	0.03	0.01	$f(u)$	$f(u)$	1.0
Z_0 (m)	SC 3	0.9	2.65	0.80	0.95	1.15	0.05	0.02	0.04	0.03	0.1	0.02	0.01	$f(u)$	$f(u)$	1.0
	SC 4	0.9	2.65	0.55	0.55	1.15	0.02	0.02	0.04	0.03	0.1	0.02	0.01	$f(u)$	$f(u)$	1.0
	SC 5	0.8	2.65	0.60	0.75	1.15	0.05	0.05	0.04	0.03	0.1	0.03	0.01	$f(u)$	$f(u)$	1.0
	SC 1	2.0	5.0	2.0	5.0	5.0	2.0	2.0	na	na	10.0	10.0	na	na	na	10.0
	SC 2	2.0	5.0	2.0	5.0	5.0	2.0	2.0	na	na	10.0	10.0	na	na	na	10.0
A (mm)	SC 3	2.0	5.0	5.0	10.0	5.0	5.0	5.0	na	na	10.0	10.0	na	na	na	10.0
	SC 4	2.0	5.0	5.0	10.0	5.0	5.0	5.0	na	na	10.0	10.0	na	na	na	10.0
	SC 5	2.0	5.0	2.0	5.0	5.0	2.0	2.0	na	na	10.0	10.0	na	na	na	10.0
α		1.0	0.6	1.1	0.8	0.8	1.2	1.2	50.0	50.0	1.3	2.0	50.0	100.0	100.0	1.5
γ		0.56	0.58	0.56	0.56	0.56	0.54	0.54	0.54	0.54	0.54	0.54	0.54	0.50	0.50	0.56

*Note: $f(u)$ represents a function of wind speed (u) and na represents not applicable.

Figure 5: Reproduction of Table 3 from (Zhang, Gong, Padro, & Barrie, 2001).

This now fully defines the model of Zhang. The primary advantage of Zhang is the model is parameterized to specific landuse categories that are typically available in landuse databases used in atmospheric weather models. The model of Zhang also nicely defines the A_{veg} parameter which was essentially unknowable with Slinn. Unfortunately, Zhang introduces the complexity of having to iteratively solve for the Monin-Obukhov length, know the relative humidity, landuse category, and season of year to solve for the appropriate deposition velocity. These are simple problems for an operational weather model running regional forecasts with access to a landuse database. It is a non-trivial issue to someone performing a point calculation on sample data taken in the field.

3.3.2.2. Bin Model

Zhang[104] in the development of their model noted the complexity of trying to implement a particle size specific model for weather models that often only track specific bins of particle sizes and not individual sizes or arbitrary distributions. As noted before, these bins are typically only three in number. These being nuclei, accumulation, and coarse bins. Zhang[105] refers to these as fine, coarse, and giant modes and defines their distribution as found in Table 2.

Table 2: Particle Size Distribution information for bins used in (Zhang & He, 2014).

Bin	Mass Median Diameter(μm)	Geometric Standard Deviation	Weighted Settling Velocity (m s^{-1})
Fine	2.5	2.2	3.7e-5
Coarse	4.5	1.6	1.8e-3
Giant	20	1.6	3.4e-2

In the bin model, Zhang then integrated over these distributions to develop a distribution weighted settling velocity. The value for this distribution weighted settling velocity is found in Table 2.

The formula for deposition velocity was then developed using the algorithms from the size specific model[106] for each of the bins. Formulas for each bin follow.

The deposition velocity for the fine particles is defined as

* MERGEFORMAT [3.53]

$$V_{d,f} = V_{s,f} + \frac{1}{R_a + R_{b,f}}$$

where

- $V_{d,f}$ is the deposition velocity of fine particles.
- $V_{s,f}$ is the settling velocity of fine particles from Table 2.

[104] (Zhang & He, 2014)
[105] Ibid.
[106] (Zhang, Gong, Padro, & Barrie, 2001)

- $R_{b,f}$ is the quasi-laminar and resistance term for fine particles which is defined by the equation

* MERGEFORMAT [3.54]

$$R_{b,f} = \frac{1}{a_1 u_*}$$

where

- a_1 is a coefficient of fit by landuse category and displayed in Figure 6

The a_1 values were calculated using regression analysis upon the calculation of R_b values from the Petroff and Zhang model[107] for each landuse category and a statistical spread of the other calculation parameters.

Table 1. The original land use categories (LUCs) and their regrouping for the new algorithm for $V_{ds}(PM_{2.5})$. Empirical constant a_1 for use in Eq. (4) is provided.

Original LUC no.	LUC definition	New group no.
01	water	5
02	ice	2
03	inland lake	5
04	evergreen needleleaf trees	2
05	evergreen broadleaf trees	2
06	deciduous needleleaf trees	2
07	deciduous broadleaf trees	2
08	tropical broadleaf trees	1
09	drought deciduous trees	2
10	evergreen broadleaf shrub	3
11	deciduous shrubs	3
12	thorn shrubs	4
13	short grass and forbs	4
14	long grass	3
15	crops	4
16	rice	4
17	sugar	4
18	maize	3
19	cotton	4
20	irrigated crops	4
21	urban	2
22	tundra	2
23	swamp	4
24	desert	2
25	mixed wood forests	2
26	transitional forest	2

New group	Original LUC no.	a_1 in Eq. (4)
1	08	3.4×10^{-3}
2	02, 04, 05, 06, 07, 09, 21, 22, 24, 25, 26	4.3×10^{-3}
3	10, 11, 14, 18	4.8×10^{-3}
4	12, 13, 15, 16, 17, 19, 20, 23	5.4×10^{-3}
5	01, 03	6.9×10^{-3}

Figure 6: Reproduction of Table 1 from (Zhang & He, 2014).

[107] (Petroff & Zhang, 2010)

The formula for the deposition velocity of coarse particles is

* MERGEFORMAT [3.55]

$$V_{d,c} = V_{s,c} + \frac{1}{R_a + R_{b.c}}$$

where

- $V_{d,c}$ is the deposition velocity of coarse particles
- $V_{s,c}$ is the settling velocity of coarse particles
- LAI is the specified leaf area index
- LAI_{max} is the maximum LAI for the specified landuse category
- $R_{b,c}$ is the quasi-laminar and surface resistance term for coarse particles defined by the equation

* MERGEFORMAT [3.56]

$$R_{b,c} = \frac{1}{\left(\sum_{i=1}^{3} b_i u_*^i\right) e^{\left(\frac{LAI}{LAI_{\max}-1}\right)\sum_{i=1}^{3} c_i u_*^i}}$$

where

- b_i and c_i are coefficients of fit displayed in Figure 7

The b, c, d, and f coefficients were all determined in a similar manner to the a coefficients for each landuse category. The Petroff and Zhang model[108] was run over a statistical distribution of input parameters using the coarse particle size distribution from Table 2 for each landuse category to develop a distribution of $R_{b,c}$ values that were then fitted using regression analysis. Values for LAI, and LAI_{max} come from Petroff[109].

Table 2b. Empirical constants for use in Eqs. (8) and (11) for Category 2 LUCs.

	$V_{ds}(PM_{2.5-10})$						$V_{ds}(PM_{10+})$					
LUC	b_1	b_2	b_3	c_1	c_2	c_3	d_1	d_2	d_3	f_1	f_2	f_3
06: deciduous needleleaf trees	-1.2×10^{-1}	1.2×10^{0}	7.1×10^{-1}	4.8×10^{0}	-5.1×10^{0}	1.8×10^{0}	-1.6×10^{0}	6.6×10^{1}	-1.7×10^{1}	7.7×10^{0}	-1.5×10^{1}	7.8×10^{0}
07: deciduous broadleaf trees	1.6×10^{-2}	3.4×10^{-1}	4.5×10^{-1}	1.8×10^{0}	-2.0×10^{-1}	-5.3×10^{-1}	-2.2×10^{0}	3.9×10^{1}	-6.7×10^{0}	6.2×10^{0}	-1.2×10^{1}	6.1×10^{0}
11: deciduous shrubs	5.6×10^{-2}	1.6×10^{-1}	2.8×10^{-1}	7.4×10^{-1}	1.7×10^{0}	-1.4×10^{0}	-2.2×10^{0}	2.7×10^{1}	-2.7×10^{0}	7.7×10^{0}	-1.4×10^{1}	7.4×10^{0}
14: long grass	-7.9×10^{-2}	1.0×10^{0}	6.6×10^{-1}	5.1×10^{0}	-4.2×10^{0}	9.9×10^{-1}	-2.0×10^{0}	6.3×10^{1}	-1.6×10^{1}	1.1×10^{1}	-2.0×10^{1}	1.1×10^{1}
15: crops	-6.0×10^{-2}	1.0×10^{0}	6.5×10^{-1}	3.4×10^{0}	-2.4×10^{0}	3.4×10^{-1}	-2.0×10^{0}	6.2×10^{1}	-1.5×10^{1}	7.9×10^{0}	-1.5×10^{1}	8.0×10^{0}
16: rice	-6.0×10^{-2}	1.0×10^{0}	6.5×10^{-1}	3.2×10^{0}	-2.1×10^{0}	2.3×10^{-1}	-2.0×10^{0}	6.2×10^{1}	-1.5×10^{1}	7.7×10^{0}	-1.5×10^{1}	7.8×10^{0}
17: sugar	7.5×10^{-2}	1.2×10^{-1}	2.4×10^{-1}	3.6×10^{-1}	1.6×10^{0}	-1.1×10^{0}	-2.1×10^{0}	2.4×10^{1}	-1.8×10^{0}	6.5×10^{0}	-1.2×10^{1}	6.3×10^{0}
18: maize	5.6×10^{-2}	1.6×10^{-1}	2.8×10^{-1}	6.6×10^{-1}	1.4×10^{0}	-1.1×10^{0}	-2.2×10^{0}	2.7×10^{1}	-2.6×10^{0}	6.5×10^{0}	-1.2×10^{1}	6.3×10^{0}
19: cotton	7.5×10^{-2}	1.2×10^{-1}	2.4×10^{-1}	3.6×10^{-1}	1.6×10^{0}	-1.1×10^{0}	-2.1×10^{0}	2.4×10^{1}	-1.8×10^{0}	6.5×10^{0}	-1.2×10^{1}	6.3×10^{0}

Figure 7: Reproduction of Table 2b from (Zhang & He, 2014).

[108] Ibid.
[109] Ibid.

The equation for the deposition of giant particles is

* MERGEFORMAT [3.57]

$$V_{d,g} = V_{s,g} + \frac{1}{R_a + R_{b.g}}$$

where

- $V_{d,g}$ is the deposition velocity of giant particles
- $V_{s,g}$ is the settling velocity of giant particles
- $R_{b,g}$ is the quasi-laminar and surface resistance term for giant particles defined by the equation

* MERGEFORMAT [3.58]

$$R_{b,g} = \frac{1}{\left(\sum_{i=1}^{3} d_i u_*^i\right) e^{\left(\frac{LAI}{LAI_{\max}-1}\right)\sum_{i=1}^{3} f_i u_*^i}}$$

where

- d_i and f_i are coefficients of fit displayed in Figure 7

This completes the definition of the Zhang bin model. The model is designed to work well for atmospheric models that generally only track bulk categories of particles and not specific sizes. The deposition velocity for any arbitrary particle size distribution can be calculated by determining the fraction of the distribution within each of the bins and then multiplying the bin settling velocity by the fraction in the bin and summing over the bins. However, this model assumes a particle size distribution that may not match the actual distribution of the source being modeled or measured. Zhang addressed this issue by performing a sensitivity analysis to the particle size distributions. They found that the overall deposition velocity changed by up to a factor of 2 for reasonable shifts in particle size distributions from one bin to another. Thus the model was generally not over sensitive to the actual versus assumed distribution.

The primary issues with this bin model are similar to those of the original Zhang model. There is still a need to recursively solve R_a and L which now comes from the more complicated definition of Petroff and Zhang. This formulation will be discussed in the next section. Furthermore, the bin model now requires the introduction of an essentially unknowable leaf area index (LAI) value, although a range of valid values per land use category is available[110]. The bin model does expand upon the arbitrary particle size model by introducing 26 instead of 16 land use categories.

[110] Ibid.

3.3.3. *Description of Petroff and Zhang*

The model of Petroff and Zhang is the most recent and complete of all the models of the Slinn family. It is also the most complicated. Petroff and Zhang expanded the land use categories available from for use from the sixteen categories in Zhang to twenty six, thus generalizing the model to more surface types.

Deposition velocity in the Petroff and Zhang model is defined at a specified reference height (z_o) as

* MERGEFORMAT [3.59]
$$V_d\left(Z_r\right)=\begin{pmatrix} V_{drift}+\dfrac{1}{R_a(z_o,Z_r)+\dfrac{1}{V_{ds}}} \\ V_{drift}+\dfrac{1}{R_a(z_o,Z_r)+\dfrac{1}{E_g u_*}} \end{pmatrix}\begin{pmatrix} Vegetated \\ Non-Vegetated \end{pmatrix}$$

where

- V_{drift} replaces V_s as the settling velocity and include other drift (phoretic) effects

V_{drift} is defined as

* MERGEFORMAT [3.60]
$$V_{drift}=V_s+V_{phor}$$

where

- V_{phor} is the velocity of phoretic effects which is defined as 5e-5 m s^{-1} for land use categories 1-3,23, and 0 otherwise

R_a is defined as

* MERGEFORMAT [3.61]
$$R\left(z_o,Z_r\right)=\frac{1}{ku_*}\begin{pmatrix} \ln\left(\dfrac{Z_r-d_c}{z_0-d_c}\right)-\psi_h\left(\dfrac{Z_r-d_c}{L_m}\right)-\psi_h\left(\dfrac{z_o-d_c}{L_m}\right) \\ \ln\left(\dfrac{Z_r-d_c}{z_0}\right)-\psi_h\left(\dfrac{Z_r-d_c}{L_m}\right)-\psi_h\left(\dfrac{z_o}{L_m}\right) \end{pmatrix}\begin{pmatrix} Vegetated \\ Non-Vegetated \end{pmatrix}$$

where

- d_c is the canopy height

ψ_h is the integrated stability function for heat which is defined as

* MERGEFORMAT [3.62]
$$\psi_h = \begin{pmatrix} 2\ln\left(0.5\left(1+\sqrt{1-16x}\right)\right) \\ 5x \end{pmatrix} \begin{pmatrix} x \in [-2,0] \\ x \in [0,1] \end{pmatrix}$$

V_{ds} which is the velocity into the surface is defined as

* MERGEFORMAT [3.63]
$$V_{ds} = u_* E_g \left(\frac{1+\left(\frac{Q}{Q_g}-\frac{\alpha}{2}\right)\left(\frac{\tanh(\eta)}{\eta}\right)}{1+\left(Q_g-\frac{\alpha}{2}\right)\left(\frac{\tanh(\eta)}{\eta}\right)} \right)$$

where

- E_g is the ground deposition efficiency
- Q is a nondimensional relation between the turbulent transport time scale and the vegetation collection time scale
- Q_g is analogous to Q, but for the ground
- η is defined by the equation

* MERGEFORMAT [3.64]
$$\eta = \sqrt{\frac{\alpha^2}{4}+Q}$$

where

- α is an extinction coefficient to account for the influence of the canopy on flow stability and defined by the equation

* MERGEFORMAT [3.65]
$$\alpha = \left(\frac{k_x LAI}{12k^2\left(1-\frac{d}{h}\right)^2} \right)^{\frac{1}{3}} \phi_m^{\frac{2}{3}}\left(\frac{h-d}{L_m}\right)$$

where

- k_x is a coefficient to account for inclination angle of the canopy to the flow and not further defined
- h is the mean height of the canopy
- LAI is the leaf area index for the land use category
- φ_m is the non-dimensional stability function for momentum and defined by the equation

* MERGEFORMAT [3.66]
$$\phi_m = \begin{pmatrix} (1-16x)^{\frac{-1}{4}} \\ 1+5x \end{pmatrix} \begin{pmatrix} x \in [-2,0] \\ x \in [0,1] \end{pmatrix}$$

The definition of Q is

* MERGEFORMAT [3.67]
$$Q = \frac{h * LAI * V_t}{K_p}$$

where

- K_p is the aerosol eddy diffusivity defined as

* MERGEFORMAT [3.68]
$$K_p = \frac{ku_* (h-d)}{\phi_h \left(\frac{h-d}{L_m} \right)}$$

where

- φ_h is the stability function for heat defined as

* MERGEFORMAT [3.69]
$$\phi_h = \begin{pmatrix} \sqrt{1-16x} \\ 1+5x \end{pmatrix} \begin{pmatrix} x \in [[-2,0] \\ x \in [0,1] \end{pmatrix}$$

Q_g is defined as

* MERGEFORMAT [3.70]
$$Q_g = \frac{hV_s}{K_p}$$

Finally, E_g is defined as

* MERGEFORMAT [3.71]
$$E_g = E_b + E_{it}$$

where

- U_h is the wind velocity at height h
- E_b is the collection efficiency due to Brownian diffusion
- E_{in} is the collection efficiency due to inertial interception
- E_{im} is the collection efficiency due to inertial impaction
- E_{it} is the collection efficiency due to eddy turbulent impaction

* MERGEFORMAT [3.72] $$E_b = \frac{\left(\frac{Sc^{-\frac{2}{3}}}{14.5}\right)}{\left(\frac{1}{6}\ln\left(\frac{(1+F)^2}{1-F+F^2}\right)+\frac{1}{\sqrt{3}}\arctan\left(\frac{2F-1}{\sqrt{3}}\right)+\frac{\pi}{6\sqrt{3}}\right)}$$

where

- F is defined as

* MERGEFORMAT [3.73] $$F = \frac{Sc^{\frac{1}{3}}}{2.9}$$

E_{it} is defined as

* MERGEFORMAT [3.74] $$E_{it} = \begin{pmatrix} 0.0025C_{it}t^+ \\ C_{it} \end{pmatrix}\begin{pmatrix} t^+ < 20 \\ t^+ \geq 20 \end{pmatrix}$$

where

- C_{it} is a coefficient of fit with a value of 0.14

Table 2. Coefficients for different Land Use Categories (LUC). The obstacle shape chosen to represent the LUC is given in brackets as N for needle and L for leaf or plane obstacles.

	LUC	h (m)	z_0 (m)	d (m)	LAI 2-sides	L (cm)	C_B	C_{IN}	C_{IM}	β_{IM}	C_{IT}
1	water	–	$f(u)$	0	–	–	–	–	–	–	–
2	ice	–	0.01	0	–	–	–	–	–	–	–
3	inland lake	–	$f(u)$	0	–	–	–	–	–	–	–
4	evergreen needleleaf (N)	15	0.9	12	10	0.15	0.888	0.810	0.162	0.60	0
5	evergreen broadleaf (L)	33.33	2	26.67	12	4	1.262	0.216	0.130	0.47	0.056
6	deciduous needleleaf (N)	15	0.4–0.9	12	0.2–10	0.15	0.888	0.810	0.162	0.60	0
7	deciduous broadleaf (L)	16.67	0.4–1.	13.33	0.2–10	3	1.262	0.216	0.130	0.47	0.056
8	tropical broadleaf (L)	41.67	2.5	33.33	12	4	1.262	0.216	0.130	0.47	0.056
9	drought deciduous forest (L)	16.67	0.6	13.33	8	3	1.262	0.216	0.130	0.47	0.056
10	evergreen broadleaf shrubs (L)	1.54	0.2	0.98	6	2	0.930	0.140	0.086	0.47	0.014
11	deciduous shrubs (L)	1.54	0.05–0.2	0.98	1–6	2	0.930	0.140	0.086	0.47	0.014
12	thorn shrubs (L)	1.54	0.2	0.98	6	2	0.930	0.140	0.086	0.47	0.014
13	short grass and forbs (N/L)	0.31	0.04	0.20	2	0.5	0.700/ 0.996	0.700/ 0.191	0.191/ 0.191	0.60/ 0.47	0.042/ 0.042
14	long grass (L)	0.15–0.77	0.02–0.10	0.10–0.49	1–4	1	0.996	0.162	0.081	0.47	0.056
15	crops (L)	0.15–0.77	0.02–0.10	0.10–0.49	0.2–8	3	0.996	0.162	0.081	0.47	0.056
16	rice (L)	0.15–0.77	0.02–0.10	0.10–0.49	0.2–12	2	0.996	0.162	0.081	0.47	0.056
17	sugar (L)	0.15–0.77	0.02–0.10	0.10–0.49	0.2–10	4	0.996	0.162	0.081	0.47	0.056
18	maize (L)	0.15–0.77	0.02–0.10	0.10–0.49	0.2–8	5	0.996	0.162	0.081	0.47	0.056
19	cotton (L)	0.15–1.54	0.02–0.2	0.10–0.98	0.2–10	7	0.996	0.162	0.081	0.47	0.056
20	irrigated crops (L)	0.38	0.05	0.25	10	3	0.996	0.162	0.081	0.47	0.056
21	urban (N/L)	17	1	11.90	1	0.15/3	0.888/ 1.262	0.810/ 0.216	0.162/ 0.130	0.60/ 0.47	0/ 0.056
22	tundra (N)	0.23	0.03	0.14	0.2–4	0.5	0.700	0.700	0.191	0.60	0.042
23	swamp (L)	0.77	0.1	0.49	8	0.2–4	0.996	0.162	0.081	0.47	0.056
24	desert	–	0.04	–	0	–	–	–	–	–	–
25	mixed wood forest* (N/L)	15	0.6–0.9	12	6–10	0.15/3	0.888/ 1.262	0.810/ 0.216	0.162/ 0.130	0.60/ 0.47	0/ 0.056
26	transitional forest* (N/L)	15	0.6–0.9	12	6–10	0.15/3	0.888/ 1.262	0.810/ 0.216	0.162/ 0.130	0.60/ 0.47	0/ 0.056

* For the mixed wood forest and transitional forest, the deposition velocity for the evergreen needleleaf forest (LUC 4) and for the deciduous broadleaf forest (LUC 7) are calculated and the resulting deposition velocity for the mixed wood forest and the transitional forest is estimated as the average weighted by the proportion of tree types.

1350

Figure 8: Reproduction of Table 2 from (Petroff & Zhang, 2010) containing all model parameters for each landuse category.

The model of Petroff and Zhang is clearly the most complicated of all models so far discussed with terms to account for orientation of vegetative surfaces to the flow, mean canopy height, canopy depth, attenuation of flow due to the canopy, and more. However, Figure 9 is just one example that shows this model is at best marginally better than any other model previously devised. The area where it and the far simpler Zhang model disagree with field measurements is simply shifted. Indeed, in their paper[111] the authors themselves note that the model underestimates the deposition velocity of intermediate particles by a factor of 6, whereas the original Zhang model is only off by a factor of 10. Thus, the two models have essentially the same error, it is merely shifted in particle size spectrum. This is the criticism that has already been leveled against all the various models earlier, that they are all off by an order of

[111] (Petroff & Zhang, 2010)

magnitude or more in some area of the particle size spectrum, with the primary area of disagreement being the critical intermediate particle region.

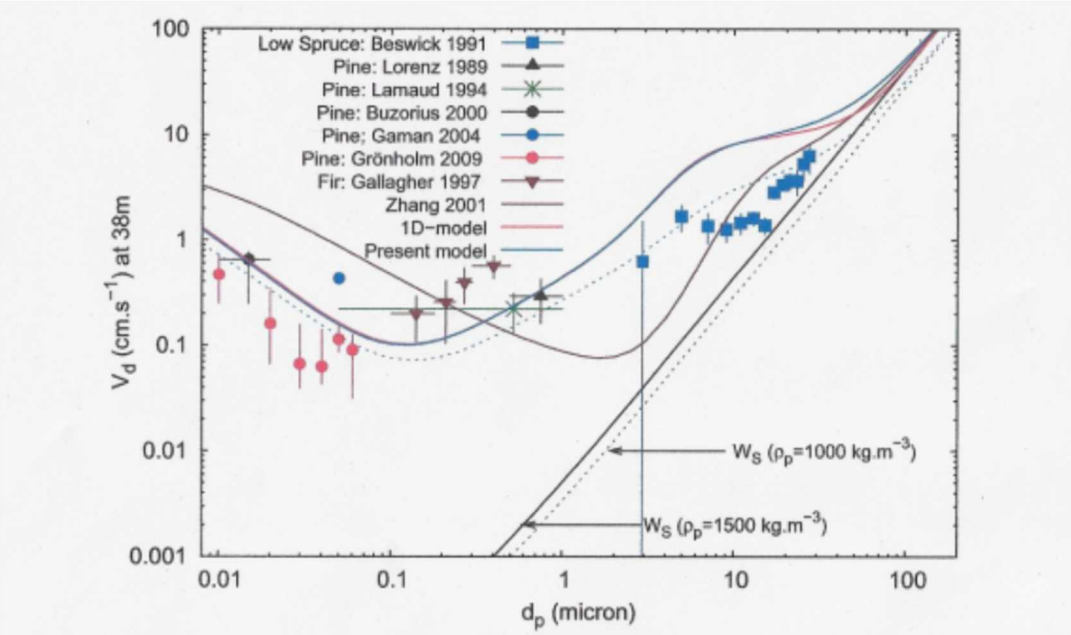

Fig. 5. Deposition on coniferous forest, as measured by Beswick et al. (1991); Lorenz and Murphy (1989); Lamaud et al. (1994); Buzorius et al. (2000); Gaman et al. (2004); Grönholm et al. (2009); Gallagher et al. (1997). A friction velocity of 47.5 cm s^{-1}, a particle density of 1500 kg m^{-3} and the parameters of the LUC 4 are used to run the model of Zhang et al. (2001, in plain brown), the 1-D-model (in plain red) and the present model (in plain blue). Are added in blue dots the predictions of the present model obtained under the configuration of Beswick et al.'s spruce: h=4.2 m, h_c=1 m, LAI=10, z_0=0.3 m and d=2.8 m, ρ_p=1000 kg m^{-3}. All deposition velocities are re-calculated at z_R=38 m.

Figure 9: Reproduction of Figure 5 from (Petroff & Zhang, 2010).

3.3.4. Issues Surrounding Data

Before comparing the Slinn family of models, it is important to discuss the dataset to which these models are so heavily fitted. All of these models were fitted to field data taken over various specific surfaces, generally in remote area where the vegetative cover was sufficiently uniform for a "sufficiently" long upwind fetch and a "sufficient" distance from any pollutant source. All data collection was typically performed at heights on the order of 10s of meters, generally eighteen to thirty meters. All used micrometeorological techniques to measure air concentrations.

These micrometeorological techniques aim to measure the vertical turbulent flux above the canopy and assume homogeneity in time and space, with no ongoing source of particulate so that turbulent flux can be related to deposition flux[112]. But turbulent deposition experiments are difficult to perform with accuracy, even under the controlled conditions of a wind tunnel. In the field critical values of particle size,

[112] (Petroff, Mailliat, Ameilh, & Anselmet, 2008)

shape, density, and total mass are uncontrolled and spatially and temporally inhomogeneous[113]. Furthermore, to extrapolate these field measurements to new situations requires similitude between vegetative environment, fetch, pollutant, plume shape, particle shape, density, diameter, wind profile and more[114]. A further limitation is the data itself is generally restricted to purely neutral conditions[115].

Beyond this, the corrections made to the micrometeorological flux data that is collected are generally on the same order of magnitude or more than the actual data collected[116]. These corrections are also not uniform between studies, and those that should be preferred or are actually applicable have not been agreed upon by the particle flux community[117], and thus are applied differently and somewhat arbitrarily from study to study.

The accuracy of the collected data is also highly dependent on the counting statistics of the instruments which themselves cannot account for particle shape[118]. This is significant because particle size counts are used to calculate deposition velocity as a function of particle size. Yet because of instrument limitations, the actual particle size, density, and shape are significantly uncertain, leading to great uncertainty in the use and applicability of the field data in defining model parameters[119]. This limits the applicability of most field data to diameters of less than 0.1 μm, a region where most models predict well and agree closely[120].

Another issue with field data is the measurement of the deposited concentration of material. The particle flux of large particles dominates the deposition velocity calculation because these particles, although small in number, contain a disproportionate fraction of the deposited mass[121]. Hence, the presence of a small number of large particles greatly enhances the deposited mass[122]. However, these large particles are not measurable by the micrometeorological techniques and instruments for airborne flux data. This results in a substantial increase in deposited mass and a lack of recording of airborne mass, leading to deposition velocities that appear to be substantially higher than those recorded in wind tunnel studies.

All of the issues presented call into great questionability the applicability of data used to derive the fits in the Slinn family of models. These fits are heavily to exclusively dependent on field measurement data that is known to be of highly questionable quality, data for which the error bars equal or exceed the data. It has well been stated,

---

[113] (Noll & Fang, Development of a Dry Deposition Model For Atmospheric Coarse Particles, 1989)
[114] (Sehmel & Hodgson, A Model for Predicting Dry Deposition of Particles and Gases to Environment Surfaces - PNL-SA-6721, 1978)
[115] (Petroff, Mailliat, Ameilh, & Anselmet, 2008)
[116] (Pryor, Larsen, Sorensen, & Barthelmie, Particle Fluxes Above Forests: Observations, Methodological Considerations, and Method Comparisons, 2008)
[117] Ibid.
[118] Ibid.
[119] (Petroff, Mailliat, Ameilh, & Anselmet, 2008)
[120] (Pryor, Larsen, Sorensen, & Barthelmie, Particle Fluxes Above Forests: Observations, Methodological Considerations, and Method Comparisons, 2008)
[121] (Lin, Noll, & Holsen, 1994)
[122] (Noll & Fang, Development of a Dry Deposition Model For Atmospheric Coarse Particles, 1989)

"Given the persistence of aged formulations, and the wide acceptance of basic datasets that now appear to be of questionable relevance to the case of the model grid cell, it is surely time for new and highly advanced measurement capabilities in field studies to find solutions convincing to all."[123]

Given the discussion thus far, the data upon which the Slinn family of models rest must be an important consideration when considering which model to choose.

3.3.5. Comparison

For the Slinn and Slinn family, several models have been described. They include the original model of Slinn; the original model of Zhang; both its original arbitrary particle size distribution variant, and the later particle bin model that was based on the later Zhang and Petroff model; and the most advanced model of Petroff and Zhang. The purpose of this section is to compare these models within their own family. An overall comparison of the Slinn family with the models from the Sehmel family will follow after discussing the implementation currently in use by NARAC.

Figure 10 is a reproduction of Figure 7 from (Hicks, Saylor, & Baker, 2016) that takes a wide swath of data from numerous field studies for forested areas and compares them to predictions from a set of models from the Slinn family. Note that Nho-Kim and Pleim and Ran were not discussed here but are of similar set up and complexity to those models that were previously discussed. From the figure it is easy to see that which of the models is "best" is surely a matter of perspective, and the performance of them all in the range of approximately 0.1 to 10 μm is generally within an order of magnitude, albeit low compared to field data.

[123] (Hicks, Saylor, & Baker, 2016)

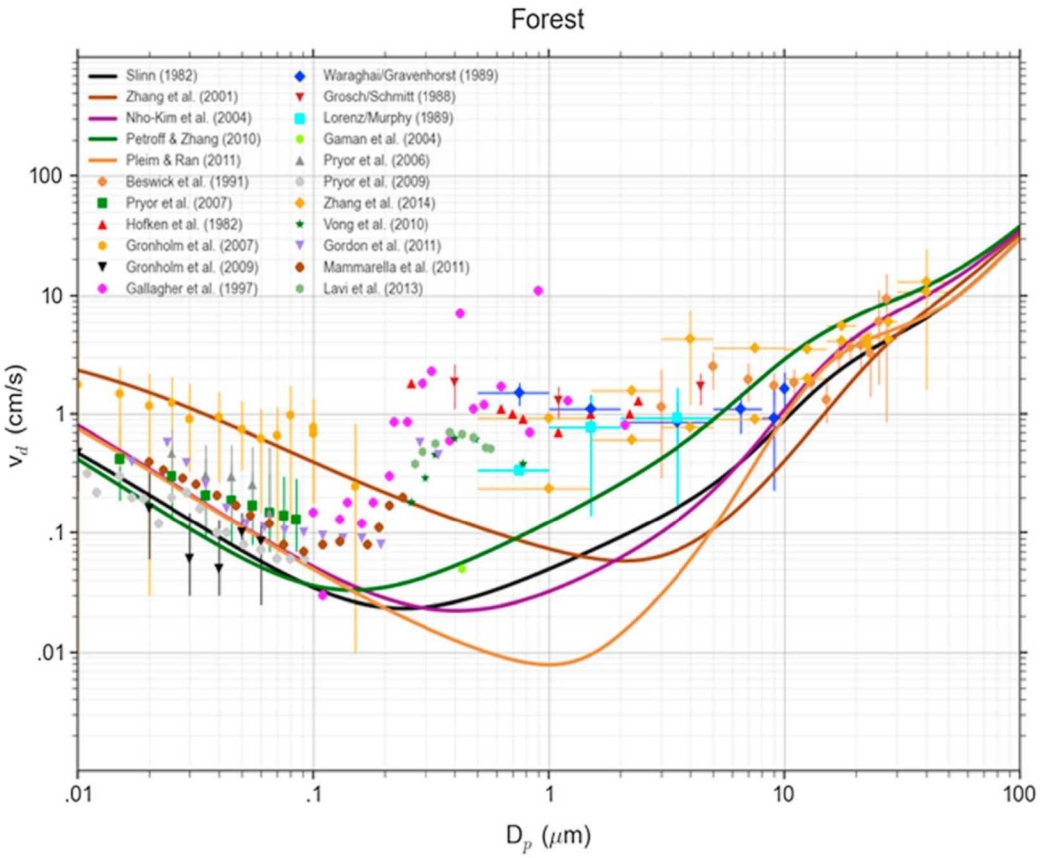

Figure 7. The dependence of the particle deposition velocity from the air to forest canopies, as predicted by several modeling schemes (the lines) and as determined by field experiments (the points). Note that the models seem to share the familiar "well" in the curve, whereas almost all of the experimental data do not.

Figure 10: Reproduction of Figure 7 from (Hicks, Saylor, & Baker, 2016)

Over the range of particles sizes for which data is shown in Figure 10, the models of Nho-Kim and Petroff and Zhang appear qualitatively to capture the broad range the best. With Nho-Kim outperforming in the outlier regions, and Petroff and Zhang performing better, although still poorly, in the critical 0.1 to 10 µm range. Although not shown, all the models generally perform better for landuse categories that are not as rough as forests for which the data in Figure 10 is valid.

Which of these models is the best, and why? This turns out to be a complicated question. Using Figure 10 it would appear to be either Petroff and Zhang or Nho-Kim. Using Figure 9—it could just as easily be the original Zhang model—the original Slinn model almost never outperforms its descendants. The question ultimately comes down to how the model is going to be used, into what environment it is going to be placed, and what particles sizes are part of the problem.

If regional scale modeling with a landuse database and a well-formed methodology for iteratively solving for the Monin-Obukhov length exists, the Petroff and Zhang or Nho-Kim models will be the best choices to date. Of these Petroff and Zhang is currently the most widely used and adopted by the community. However, for other

surfaces, such as snow, the original Zhang model does just as well and is not as complicated as the Petroff and Zhang model. All models, not surprisingly before best when compared to the data actually used to fit them.

4. CURRENT NARAC IMPLEMENTATION

NARAC in 2013-2015 performed its own investigation into the issue of deposition modeling through a series of reports[124,125,126,127]. NARAC determined that the model of Petroff and Zhang was the most "advanced and current approach"[128] for calculating dry deposition velocities for particles. They found the model to be appropriate for integration into the NARAC modeling system.

The reasoning cited for their choice are that the model of Petroff and Zhang represents a "major advance from earlier dry deposition models due to the inclusion of recent experimental data in formulating landuse dependent parameterizations"[129]. They note that Petroff and Zhang has been validated against observations made after the model had been completed. They further note that Petroff and Zhang have several features that "make it ideal for integration into a real-time emergency response modeling system."[130] These features being; fast runtime that has little impact on overall runtime, parameterizations to account for a range of vegetative surfaces, only requires meteorological variables that are readily available from numerical weather prediction data sets widely available to NARAC, and finally, ease of adding additional landuse categories to the dataset if they become available[131].

To fully implement the Petroff and Zhang model, NARAC took the list of landuse categories native to the model and mapped them to the landuse categories available in the Weather Research and Forecasting (WRF) model. NARAC further defaulted the faction of LAI corresponding to coniferous trees in the mixed forest types to 0.5. NARAC further adjusted the arbitrary reference heights in Petroff and Zhang from 10 meters and twice the canopy height for forests to 1.5 m and 1.5 times the canopy height[132]. No detailed reasoning for this was given in the reports. Personal correspondence with Matthew Simpson of NARAC indicated that "This specific modification was made after discussions with the model developer Petroff, who provided the code to NARAC. He used arbitrary reference heights that created issues at the boundary of lower Obukhov length values."

---

[124] Simpson, M., Belles, R., & Gowardhan, A. (2013). *Improving NARAC Accuracy by Implementation of Higher-Resolution Precipitation and Deposition Modeling* (LLNL-TR-643769). Livermore, CA: Lawrence Livermore National Laboratory.

[125] Simpson, M., Belles, R., & Walker, H. (2014). *Improving NARAC Accuracy by Implementation of Higher Resolution Precipitation and Deposition Modeling* (LLNL-TR-660754). Livermore, CA: Lawrence Livermore National Laboratory.

[126] Simpson, M., Belles, R., & Walker, H. (2014). *Improving NARAC Accuracy by Implementation of Higher-Resolution Precipitation and Deposition Modeling* (LLNL-TR-652474). Livermore, CA: Lawrence Livermore National Laboratory.

[127] Simpson, M., Belles, R., Fischer, K., & Walker, H. (2015). *Improving NARAC Accuracy by Implementation of Higher-Resolution Precipitation and Deposition Modeling* (LLNL-TR-XXXXXX). Livermore, CA: Lawrence Livermore National Laboratories

[128] (Simpson, Belles, & Walker, Improving NARAC Accuracy by Implementation of Higher-Resolution Precipitation and Deposition Modeling (LLNL-TR-652474), 2014)

[129] Ibid.

[130] Ibid.

[131] Ibid.

[132] Ibid.

Finally, the particle size space was divided into 11 particles size bins for calculation of the average deposition velocity. No details are provided in the reports on the sizes chosen, or exactly why 11 was considered reasonable other than a reference to the FLEXPART model[133,134]. Personal correspondence with Mathew Simpson of NARAC stated the following: "The number of deposition velocity bin sizes is a parameter than can be changed easily if needed based on a specific scenario. Some limited sensitivity testing showed 11 bins were able to reasonably resolve a normal distribution of particle sizes. It is always a balance between numerical cost and accuracy; we found 11 bins (as did the Flexpart model developer) to be a reasonable value to account for the range of deposition velocities at each model grid cell for each meteorological output time"

NARAC performed a series of tests which concluded in general that Petroff and Zhang reduced the deposition velocity calculated by the model by roughly one to two orders of magnitude. Commentary on the choice of Petroff and Zhang as the model of choice for the NARAC modeling system is presented in the following section.

[133] Stohl, A., Forster, C., Frank, A., Seibert, P., & Wotawa, G. (2005). "Technical Note: The Lagrangian Particle Dispersion Model FLEXPART version 6.2". *Atmospheric Chemistry and Physics, 5*, 2462-2474.
[134] Stohl, A., Sodemann, H., Eckhardt, S., Frank, A., Seibert, P., & Watawa, G. (2010). *The Lagrangian Particle Dispersion Model FLEXPART version 8.2, User Manual.*

5. ALL MODEL COMPARISON

As can be seen in this report, there is a veritable sea of deposition models to choose from with only the "best of breed" discussed in any detail. Those models fall into two general families. The family of Sehmel, and the family of Slinn and Slinn. The family of Slinn and Slinn has been far more prolific in reproducing itself into a series of ever more complicated models with ever more parameters of fit culminating in the state-of-the-art model of Petroff and Zhang. Meanwhile the Sehmel family has seen much less attention due to the lack of vegetative fitting parameters that have struck so many as essential to good prediction of deposition velocity. Yet it must be remembered from Section 2.2 that the two driving and critical factors for calculating an accurate deposition velocity are friction velocity and particle size distribution. The effects of the vegetative canopy are inherent in the turbulence, and hence the friction velocity of the flow. For all their complexity, the Slinn family of models add very little to the predictive performance of the Slinn models over the Sehmel models.

Before comparing the predictive capabilities of the models, complexity is probably the first order issue when comparing the models. It is easy to see that the models of Feng and Noel are far simpler in implementation than those of Zhang, or Petroff and Zhang. They are also far more generic. No landuse category information, or LAI, or other minute vegetative properties are needed. To implement the models, only a wind profile and an easily estimated roughness length is required.

A secondary issue surrounds the data used to derive the two family of models. The data upon which Sehmel rests is primarily wind tunnel data for which boundary and initial conditions were well controlled and for which measurements of air concentrations where take at elevations above ground level that are consistent with what FRMAC field teams would use, whereas an entire section of this report (Section 3.3.4) was dedicated to the questionability of the data upon which the Slinn family of models is based. It must be remembered that the calculated deposition velocity and hence applicable model are highly dependent on the elevation at which the air concentration data is observed. Finally, the warning of Hicks regarding the Slinn family of models deserves repeating, "Given the persistence of aged formulations, and the wide acceptance of basic datasets that now appear to be of questionable relevance to the case of the model grid cell, it is surely time for new and highly advanced measurement capabilities in field studies to find solutions convincing to all."[135] The data behind the Slinn family of models is known to be valid only for the specific conditions under which it was taken, conditions in which the initial and boundary state are not known. Is it valid to apply fits to European forests to the mangroves of Florida, or the moorlands of Scotland to the fields of the Great Plains?

All this being said, how do the best of breed Petroff and Zhang and Feng models compare to actual data? Figure 11 and Figure 12 compare the prediction of the two models to the Scottish Moorland[136]. As can be seen in these two charts, Petroff and

[135] (Hicks, Saylor, & Baker, 2016)

[136] Nemitz, E., Gallagher, M., Duyzer, J., & Fowler, D. (2002). "Micrometeorological Measurements of Particle Deposition Velocities to Moorland Vegetation". *Quarterly Journal of the Royal Meteorological Society, 128*, 2281-2300.

Zhang tend to under predict much of the moorland data by an order of magnitude while the fit of Feng is quite good. Feng in Figure 12 also reproduces settling velocities for forested areas at least as well as Petroff and Zhang do in Figure 10, and these fits are based on the four particle size bin submodel and not the more precise arbitrary particle size model.

Yet this exercise of putting up graphs of models versus data is inherently fruitless. Depending on the paper chosen, the surface type, etc., virtually every model of every family can be shown to be the best choice. So far, however, what no model has been able to capture is the sudden spike in deposition velocity at approximately 0.1 μm as seen in Figure 10. None of the models do particularly great until Petroff and Zhang at around 3 μm. Also, none of these models directly account for turbophoretic effects except for Feng. Figure 12 is a reproduction of Figure 5 from Feng. What is most noticeable from this plot is the model of Feng as friction velocity increases (surface become rougher or vegetation higher (forest)) becomes the first model to produce a sharp escalation of deposition velocity in the critical region of 0.1 μm to 1 μm. Indeed, mapping the Feng curve for the 1 m s^{-1} friction velocity over the data from Figure 10 shows a fit better than any other model with Feng reproducing the natural shape of the data curve in a way no other model comes close to with a spike in the deposition velocity in the submicron range as well as deposition velocities on the order of 1 cm s^{-1} for 1 μm particles.

The model of Feng also produces another feature seen in the data that no other model appears to be able to reproduce. This can be seen in Figure 14 where the inclusion of turbophoretic effects produces a flattening of the deposition velocity curve where other models produce a dip due to the decreased influence of Brownian diffusion before interception and impaction become important. This flattening occurs in the Feng model because particles that would normally see ever decreasing deposition velocities due to the decrease in Brownian motion instead see a flattening because turbophoretic influences increase deposition velocity in a manner commensurate to the decrease in Brownian motion, with impaction and interception eventually taking over and dominating. Turbophoretic effects increase the deposition velocity that would naturally dip as influence of Browning diffusion reduces and thereby also reduces the overall deposition velocity. Close inspection of Figure 9 through Figure 11 will show data with this flattening feature seen only in that shape of the Feng curves. All other models are either diving, or rising in the critical region, none show the ability to flatten out or spike in the critical region in the same manner as Feng.

It is this ability of Feng to reproduce the observed qualitative shape of measurement data, as well as its ability to quantitatively fit available data, that appears to show its general superiority. It further has the advantage of simplified implementation and complete general surface applicability in its favor, as well as being based on a greater spread of data for which the conditions appropriate to the data are actually known.

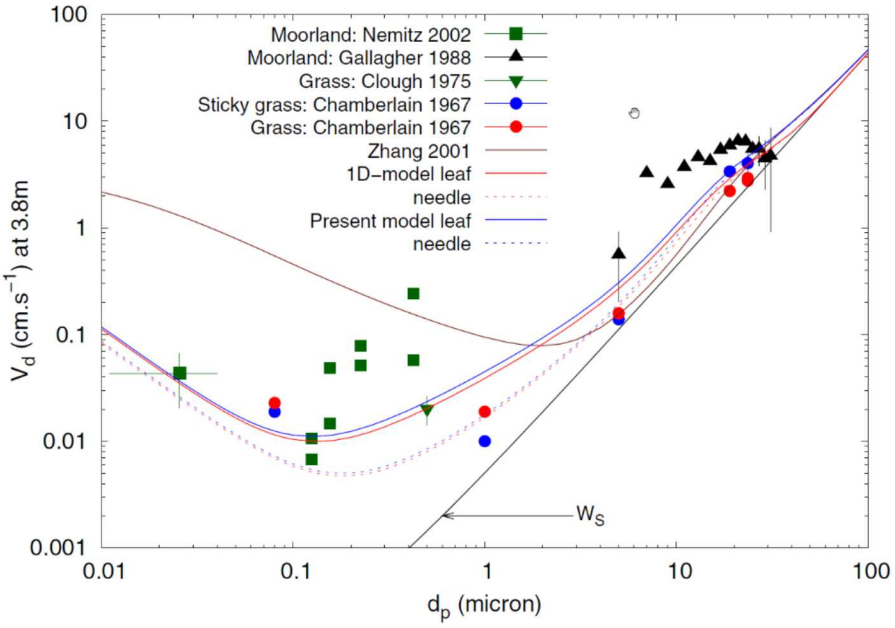

Fig. 4. Deposition on grass, as measured by Chamberlain (1967); Clough (1975); Garland (1983); Gallagher et al. (1988); Nemitz et al. (2002) for friction velocity between 25 and 55 cm s^{-1}. A friction velocity of 40 cm s^{-1} is used to run the model of Zhang et al. (2001, in brown), the 1-D-model on leaf and needle obstacles (red plain and dash) and the present model on leaf and needle obstacles (blue plain and dash). All deposition velocities are re-calculated at z_R=3.8 m. The particle density is taken as ρ_p=1500 kg m^{-3}.

Figure 11: Reproduction of Figure 4 from (Petroff & Zhang, 2010).

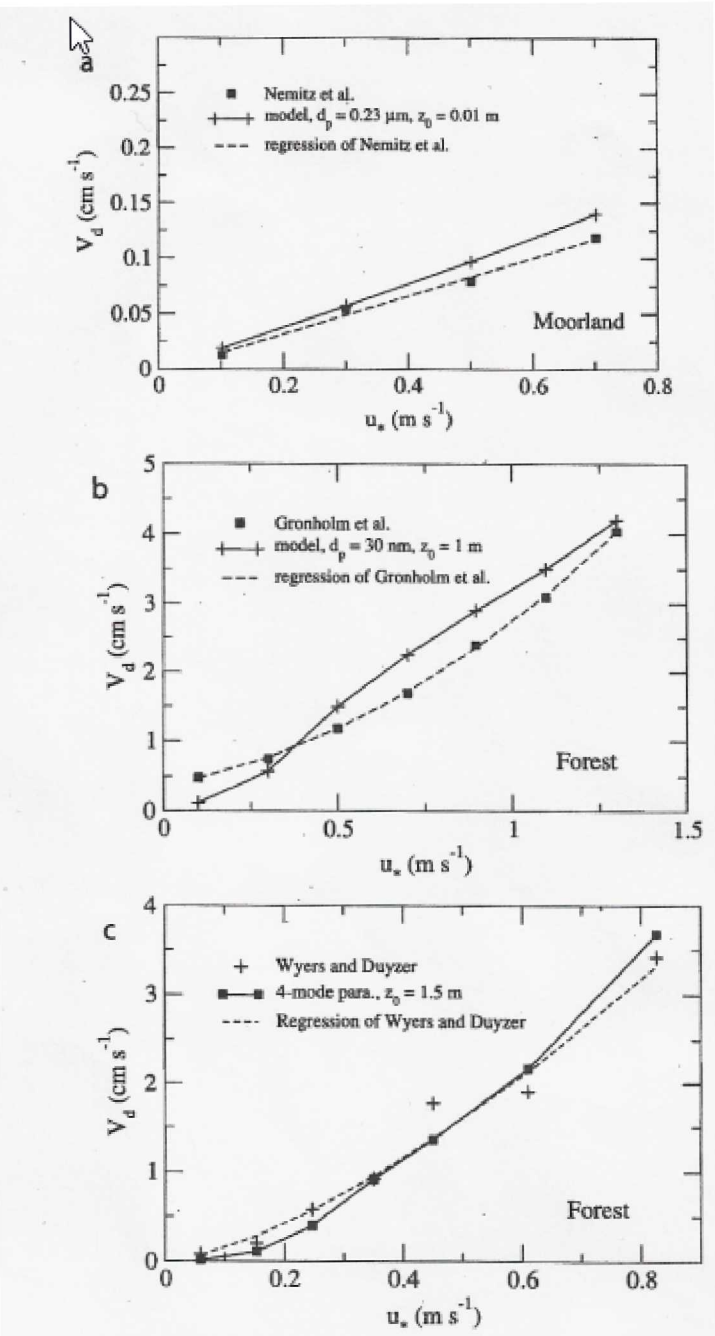

Figure 8. Comparisons of measured dry deposition velocities with predictions of the new dry deposition model and the four-mode parameterization: (a) *Nemitz et al.* [2002], (b) *Grönholm et al.* [2007], and (c) *Wyers and Duyzer* [1997].

Figure 12: Reproduction of Figure 8 from (Feng, 2008).

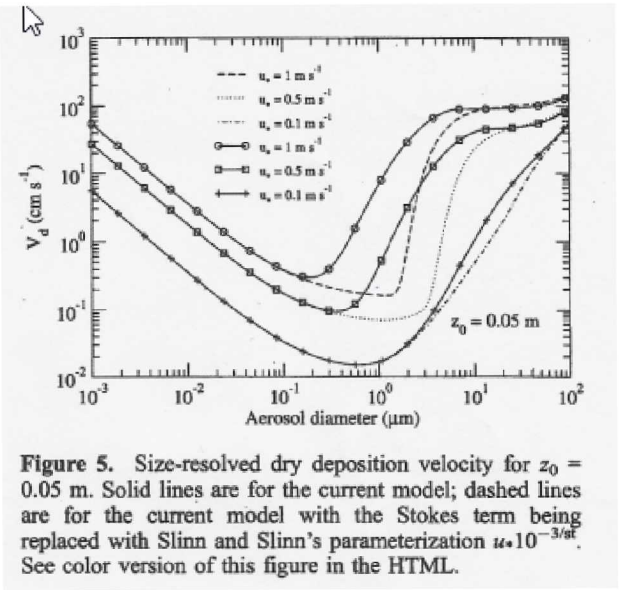

Figure 5. Size-resolved dry deposition velocity for z_0 = 0.05 m. Solid lines are for the current model; dashed lines are for the current model with the Stokes term being replaced with Slinn and Slinn's parameterization $u_* 10^{-3/st}$. See color version of this figure in the HTML.

Figure 13: Reproduction of Figure 5 from (Feng, 2008).

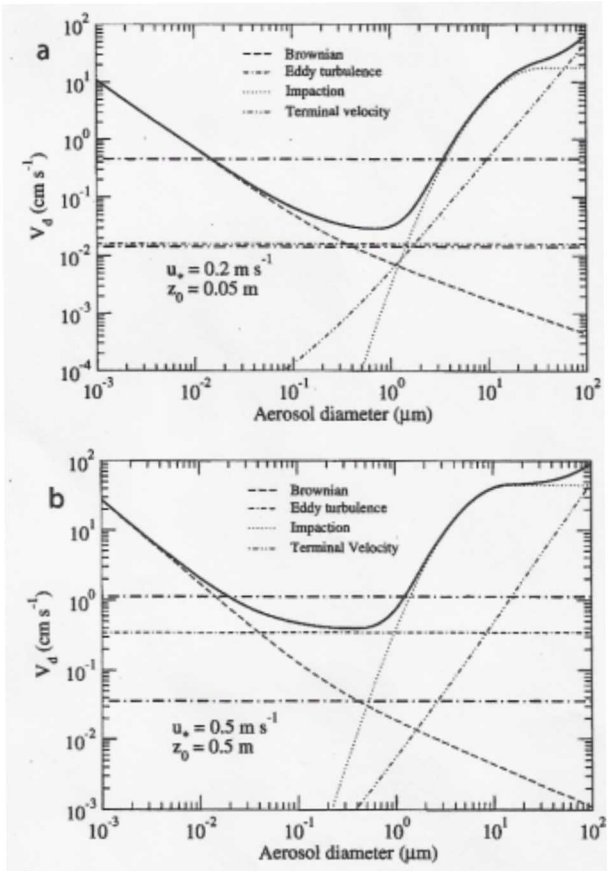

Figure 4. Size-resolved dry deposition velocities for different friction velocity and surface roughness length. The bold dot-dashed lines are the upper and lower limits of the roughness Reynolds term.

Figure 14: Reproduction of Figure 4 from (Feng, 2008).

But what of NARAC's decision to use the model of Petroff and Zhang. Again, it must be remembered the conditions under which these models were derived. Zhang, and Petroff and Zhang are good models for large vegetated areas[137], and conditions in which large regional scale roughness lengths apply[138]. These are exactly the conditions of the NARAC model. The NARAC model has access to the complicated meteorological parameters needed by Petroff and Zhang; it has access to an appropriate land use database; it is simulating the regional scale transport of pollutant; and it is simulating transport at elevations consistent with the dataset upon which Petroff and Zhang are based. Thus, for NARAC Petroff and Zhang are a very logical choice.

However, for Turbo FRMAC, Petroff and Zhang is a much less logical choice. The data requirements of the model are far beyond what makes sense to ship with Turbo FRMAC or expect the Assessment Scientists to provide. The model is based on data fits that are not as appropriate or applicable to FRMAC field measurements as the model of Feng. The Petroff and Zhang model is also far more complicated to implement than Feng and from fits to data shows not greater applicability or predictability than Feng which shows greater promise in its ability to predict flattening and sharp spikes in the submicron range than any other model. Also, as noted previously, the model of Petroff and Zhang is not recommended for the mixed urban or urban environment, a region in which it is logical for FRMAC field sample to be taken. The model of Feng has no such limitations[139]. Thus, for Turbo FRMAC, the model of Feng is considered the best choice and is also highly recommended for consideration by NARAC.

The question will logically arise as to what impact would it have for NARAC to be using Petroff and Zhang and Turbo FRMAC, Feng. This, in many ways is a difficult question to answer. NARAC is performing regional-scale to global-scale transport of pollutant using observation and forecast data to predict the broadscale deposition, resuspension, and transport of material. Turbo FRMAC is taking a field observation of ground deposition and air concentration, hopefully reasonably co-located in time and space, to predict local effects.

In general, it should not be expected that these two values will agree that well unless the localized conditions meet the broad conditions of the NARAC model reasonably well. If anything should be gleaned from this report, it is that details matter when it comes to deposition, and a regional-scale model by necessity has to dump details to produce regionally smeared results, whereas the field measurements by definition contain all the slightest of details over the very localized conditions under which the measurement was taken.

This being said, Figure 15 shows the fit of the Petroff and Zhang model to data taken by Sehmel in 1973. It can be seen that Petroff and Zhang does quite well in fitting this data. Although not shown, Feng based on Sehmel's data along with more recent work naturally fits the Sehmel data quite well also. Thus, in the region of 5 to 100 μm the

[137] (Jonsson, Karlsson, & Jonsson, 2008)
[138] (Gallagher, et al., 2002)
[139] (Mohan, 2016)

models will agree with each other quite well. From Figure 10 and other figures in this report, it can also be derived that the two models will agree within an order of magnitude of each other in most situations.

Therefore, the recommended solution which will be expounded upon in the next section is for Turbo FRMAC to use the model of Feng, whereas there is no reason for NARAC not to continue with the model of Petroff and Zhang. Although implementation of the Feng model in the NARAC modeling system as an option seems a worthy effort in unifying the two codes. This path forward enables both codes to use state-of-the-art deposition models that appear most appropriate to their use case, and which generate order of magnitude agreement with each other in deposition velocities. The use of Feng in Turbo FRMAC will also eliminate the vast discrepancy between the two current implementations wherein Turbo FRMAC is using a constant value for deposition velocity while NARAC is using a state-of-the-art, situation specific model.

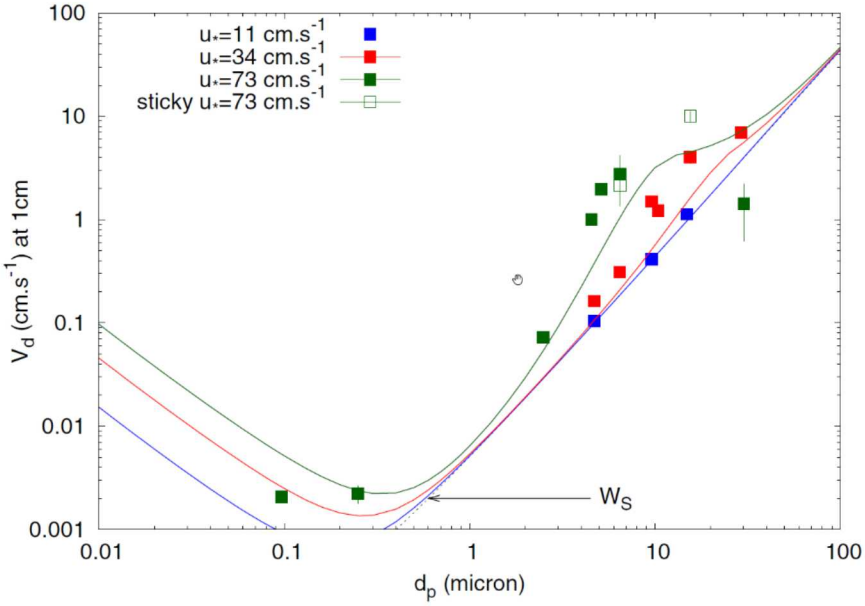

Fig. 3. Deposition on smooth soil, as measured – mean, standard deviation – by Sehmel (1973) and predicted by the present model (plain lines) for friction velocities of 11 cm s^{-1} (blue), 34 cm s^{-1} (red), 74 cm s^{-1} (green).

Figure 15: Reproduction of Figure 3 from (Petroff & Zhang, 2010).

6. PROPOSED SOLUTION

The proposed solution for Turbo FRMAC is to use the arbitrary particle size deposition model of Feng. This will require the addition of the ability for the user to import a meteorology sounding at the location of the sample and specify a roughness length. For roughness length a dropdown list of land surface type and roughness length will be provided along with the ability to specify the average height of surrounding objects in order to calculate a roughness length, since the roughness length is approximately $1/30^{th}$ the height of surrounding objects based on field studies[140].

Using the specified particle size distribution, the cumulative distribution function for that distribution will be used to calculate the next particle size such that one percent of the distribution mass is between the two particles sizes. This will be repeated until the maximum particle size is reached. For each particle size, the Feng deposition velocity will be calculated and averaged together to derive a bulk deposition velocity. Sensitivity studies will balance calculational accuracy and number of bins to derive whether one percent, ten percent, a tenth of a percent, etc., is a reasonable compromise.

For no knowledge situations, the NARAC model should be augmented to be able to produce the deposition velocity it used for a given location and time for manual entry into Turbo FRMAC or provide the deposition concentration and integrated air concentration. Turbo FRMAC will also use a no knowledge typical friction velocity[141] of 0.3 m s^{-1} to calculate deposition under nominal conditions.

[140] (Seinfeld & Pandis, 2012)

[141] Holton, J. R., & Hakim, G. J. (2013). *An Introduction to Dynamic Meteorology, Fifth Edition.* New York: Elsevier.

7. CONCLUSION

The ratio of the concentration of material in the air to the concentration of material on the ground is commonly referred to as the deposition velocity. This name is unfortunate, because it is in no means a velocity, but purely a scalar factor that happens by its definition to have units of velocity. Calculation of this term is essentially to the FRMAC as it is required to calculated emergency response values for which both the air and ground concentrations must be known, but often only one is. On the predictive size of the FRMAC, the NARAC model needs an accurate deposition velocity to calculate the transfer of airborne particulate to the ground. Meanwhile, on the field sample analysis side there is a need to calculate one concentration from the other when only one of them is known.

As was seen in this report deposition of airborne material to a depositing surface is an extremely complex process involving a wide range of processes of varying applicability across the spectrum of valid particle sizes. Thankfully, in the end, only the friction velocity and particle size distribution are truly critical to the calculation of deposition velocity.

In this paper a wide range of deposition models was examined and compared to each other. These deposition models fell into two families. The family of Sehmel, and the family of Slinn and Slinn. One model from each of these families was selected as the "best of breed." These were the Feng model from the Sehmel family and the Petroff and Zhang model from the Slinn and Slinn family.

Analysis of the data behind these models and their ability to simulate the observed shape of field measured deposition curves lead the current author to the conclusion that the Feng model was most appropriate to Turbo FRMAC, and overall the best available model. Meanwhile, NARAC came to the conclusion that that model of Petroff and Zhang was most appropriate to their situation. Both models were seen to be "best of breed", comparing well to each other. Thus, it was concluded that although it would seem applicable for NARAC to consider Feng, the agreement between the deposition models of Feng and Petroff and Zhang is sufficient enough to eliminate any requirement of universal implementation across both codes. Implementation of Feng in Turbo FRMAC will eliminate the current issue of vastly different deposition assumptions and modeling between NARAC and Turbo FRMAC and bring the two codes into alignment on this essential parameter.

Page Intentionally Blank

REFERENCES

Bach, D. H. (1979). "Particulate Transport Within Plant Canopies (II)". *Atmospheric Environment, 13*, 1681-1687.

Bagheri, G., & Bonadonna, C. (2016). "On the Drag of Freely Falling Non-Spherical Particles". *Powder Technology, 301*, 526-544.

Barati, R., Akbar, S. A., Neyshabouri, S., & Ahmadi, G. (2014). "Development of Emperical Models with High Accuracy for Estimating Drag Coefficient of Flow Around a Smooth Sphere: An Evolutionary Approach". *Powder Technology, 257*, 11-19.

Biasi, L., Reyes, A. d., Reeks, M. W., & de Santi, G. F. (2001). "Use of a Simple Model for the Interpretation of Experimental Data on Particle Resuspension in Turbulent Flows". *Aerosol Science, 32*, 1175-1200.

Cheng, N.-S. (1997). "Simplified Settling Velocity Formula for Sediment Particle". *Journal of Hydrolic Engineering*, 149-152.

Cheng, N.-S. (2009). "Comparison of Formulas for Drag Coefficients and Settling Velocities of Spherical Particles". *Powder Technology, 189*, 395-398.

Chhabra, R. P., Agarwal, L., & Sinha, N. K. (1999). "Drag on Non-Spherical Particles: An Evaluation of Available Methods". *Powder Technology, 101*, 288-295.

Chhabra, R. P., Agarwal, L., & Sinha, N. K. (1999). "Drag on Non-Spherical Particles: An Evaluation of Available Methods". *Powder Technology, 101*, 288-295.

Chien, S.-F. (1994). "Settling Velocity of Irregularly Shaped Particles". *SPE Drilling and Completion*, 281-289.

Dare, R. A. (2015). *Sedimentation of Volcanic Ash in the HYSPLIT Dispersion Model - CAWCR Technical Report No. 079.* The Centre for Australian Weather and Climate Research. Melborne: The Centre for Australian Weather and Climate Research.

Davidson, C. I., Miller, J. M., & Pleskow, M. A. (1982). "The Influence of Surface Structure on Predicted Particle Dry Deposition to Natural Grass Canopies". *Water Air Soil Pollution, 18*, 25-44.

Dioguardi, F., & Mele, D. (2015). "A New Shape Dependent Drag Correlation Formula for Non-Spherical Rough Particles: Experiments and Results". *Powder Technology, 277*, 222-230.

Donateo, A., & Contini, D. (2014). "Correlation of Dry Deposition Velocity and Fricition Velocity over Different Surfaces for PM2.5 and Particle Number Concentrations". *Advances in Meteorology*.

Erisman, J. W., Draaijers, G., Duyzer, J., Hofschreuder, P., Leeeuwen, N. V., Romer, F., Gallagher, M. (1997). "Particle Deposition to Forests - Summary of Results and Application". *Atmospheric Environment, 31*(3), 321-332.

Fang, G. C., Wu, Y. S., Chang, C. N., Chang, K. F., & Yang, D. G. (1999). "Modeling Dry Deposition of Total Particulate Mass In Trafficked and Rural Sites of Central Taiwan". *Environment International, 5*, 625-633.

Feng, J. (2008). "A Size-Resolved Model and a Four-Mode Parameterization of Dry Deposition of Atmospheric Aerosols". *Journal of Geophysical Research, 113*, D12201-.

Ferrandino, F. J., & Aylor, D. E. (1985). "An Explicit Equation for Deposition Velocity". *Boundary Layer Meteorology, 31*, 197-201.

Gallagher, M. W., Beswick, K. M., Duyzer, J., Westrate, H., Choularton, T. W., & Hummelshoj, P. (1997). "Measurement of Aerosol Fluxes to Speulder Forest Using a Micrometeorological Technique". *Atmospheric Environment, 31*(3), 359-373.

Gallagher, M. W., Nemitz, E., Dorsey, J. R., Fowler, D., Sutton, M. A., Flynn, M., & Duyzer, J. (2002). "Measurement and Parameterizations of Small Aerosol Deposition Velocities to Grassland, Arable Crops, and Forests: Influence of Surface Roughness Lenght on Deposition". *Journal of Geophysical Research, 107*(12), 8-1 to 8-10.

Ganzer, G. H. (1993). "A Rational Approach to Drag Prediction of Spherical and Non-Spherical Particles". *Powder Technology, 77*, 143-152.

Giorgi, F. (1986). "A Particle Dry Deposition Parameterization Scheme for Use in Tracer Transport Models". *Journal of Geophysical Research, 91*, 9794-9804.

Giorgi, F. (1988). "Dry Deposition Velocities of Atmospheric Aerosols as Inferred by Applying a Particle Dry Deposition Parameterization to a General Circulation Model". *Tellus, 40B*, 23-41.

Haider, A., & Levenspiel, O. (1989). "Drag Coefficient and Terminal Velocity of Spherical and Nonspherical Particles". *Powder Technology, 58*, 63-70.

Hicks, B. B., Saylor, R. D., & Baker, B. D. (2016). "Dry Deposition of Particles to Canopies-A Look Back and the Road Forward. *Journal of Geophysical Research: Atmospheres*, 14691-14707.

Holton, J. R., & Hakim, G. J. (2013). *An Introduction to Dynamic Meteorology, Fifth Edition.* New York: Elsevier.

Holzer, A., & Sommerfeld, M. (2008). "New Simple Correlation formula for the Drag Coefficient of Non-Spherical Particles". *Powder Technology, 184*, 361-365.

Hongli, Y., Minqiang, F., Airong, L., & Lianping, D. (2015). "General Formulas for Drag Coefficient and Settling Velocity of Sphere based on Theoretical Law". *International Journal of Mining Science and Technology, 25*, 219-223.

Ibrahim, M. L., Barrie, L. A., & Fanaki, F. (1983). "An Experimental and Theoretical Investigation of the Dry Deposition of Particles to Snow, Pine Trees, and Artificial Collectors". *Atmospheric Environment, 17*, 781-788.

Jonsson, L., Karlsson, E., & Jonsson, P. (2008). "Aspects of Particulate Dry Deposition in the Urban Environment". *Journal of Hazardous Materials, 153*, 229-243.

Kelessidis, V. C. (2003). "Terminal Velocity of Solid Spheres Falling in Newtonian and Non-Newtonian Liquids". *Tech. Chron. Sci.*, 43-51.

Kharchenko, A. I. (1997). "Parameterization of Dry Deposition Velocity in the Atmospheric Surface Layer". *Journal of Aerosol Science, 28*(Supplement 1), 589-590.

Lali, A. M., Khare, A. S., & Joshi, J. B. (1989). "Behavior of Solid Particles in Viscous Non-Newtonian Solutions: Settling Velocity, Wall Effects, and Bed Expansion in Solid-Liquid Beds". *Powder Technology, 57*, 39-50.

Legg, B. J., & Price, R. I. (1980). "The Contribution of Sedimentation to erosol Deposition to Vegatation with a Large Leaf Index". *Atmospheric Environment, 14*, 305-309.

Leith, D. (1987). "Drag on Nonspherical Objects". *Aerosol Science and Technology, 6*, 153-161.

Lin, J. J., Noll, K. E., & Holsen, T. M. (1994). "Dry Deposition Velocities as a Function of Particle Size in the Ambient Atmosphere". *Aerosol Science and Technology, 1994*, 239-252.

Lin, J.-M., Fang, G.-C., Holsen, T. M., & Noll, K. E. (1993). "A Comparison of Dry Deposition Modeled From Size Distribution Data and Measured With a Smooth Surface for Total Particle Mass, Lead and Calcium in Chicago". *Atmospheric Environment, 27A*(7), 1131-1138.

Loth, E. (2008). "Drag of Non-Spherical Solid Particles of Regular and Irregular Shape". *Powder Technology, 182*, 342-353.

McCready, D. I. (1986). "Wind Tunnel Modeling of Small Particle Deposition". *Aerosol Science and Technology, 5*, 301-312.

Mohan, S. M. (2016). "An Overview of Particulate Dry Deposition: Measuring Methods, Deposition Velocity, and Controlling Factors". *International Journal of Environmental Science and Technology, 13*, 387-402.

Moller, U., & Schumann, G. (1970). "Mechanisms of Transport from the Atmosphere to the Earth's Surface". *Journal of Geophysical Research, 75*(15), 3013-3019.

Nemitz, E., Gallagher, M., Duyzer, J., & Fowler, D. (2002). "Micrometeorological Measurements of Particle Deposition Velocities to Moorland Vegetation". *Quarterly Journal of the Royal Meteorological Society, 128*, 2281-2300.

Nho-Kim, E. Y., Jackson, M. M., & Oskoie, V. H. (2001). "Development of an Atmospheric Particle Dry Deposition Model". *Aerosol Science and Technology, 38*, 627-636.

Nho-Kim, E. Y., Michou, M., & Peuch, V. H. (2004). "Parameterization of Size-Dependent Particle Dry Deposition Velocities for Global Modeling". *Atmospheric Environment, 38*, 1933-1942.

Nicholson, K. W. (1988). "A Review of Particle Resuspension". *Atmospheric Environment, 22*(12), 2639-2651.

Nicholson, K. W. (1988). "The Dry Deposition of Small Particles: A Review of Experimental Measurements". *Atmospheric Environment, 22*(12), 2653-2666.

Noll, K. E., & Fang, K. Y. (1989). "Development of a Dry Deposition Model For Atmospheric Coarse Particles". *Atmospheric Environment, 23*, 585-594.

Noll, K. E., Jackson, M. M., & Oskouie, A. K. (2001). "Development of an Atmospheric Particle Dry Deposition Model". *Aeorsol Science and Technology, 35*, 627-636.

Paulson, C. A. (1970). "The Mathematical Representation of Wind Speed and Temperature Profiles in the Unstable Atmospheric Surface Layer". *Journal of Applied Meteorology, 9*, 857-861.

Pellerin, G., Maro, D., Damay, P., Gehin, E., Connan, O., Laguionie, P., Charrier, X. (2017). "Aerosol Particle Dry Deposition Velocity Above Natual Surfaces: Quantification According to the Particles Diameter". *Journal of Aerosol Science, 114*, 107-117.

Peters, K., & Eiden, R. (1992). "Modeling the Dry Deposition Velocity of Aerosol Particles to a Spruce Forest". *Atmospheric Environment, 26*, 2555-2564.

Petroff, A., & Zhang, L. (2010). "Development and Validation of a Size-Resolved Particle Dry Deposition Scheme For Applications in Aerosol Transport Models". *Geoscience Model Development Discussions, 3*, 1317-1357.

Petroff, A., Mailliat, A., Ameilh, M., & Anselmet, F. (2008). "Aerosol Dry Deposition on Vegetative Canopies, Part I: Review of Present Knowledge". *Atmospheric Environment, 42*, 3625-3653.

Petroff, A., Mailliat, A., Amielh, M., & Anselmet, F. (2008). "Aerosol Dry Deposition on Vegetative Canopies: Part II: A new Modeling Approach and Applications". *Atmospheric Environment, 42*, 3654-3683.

Pryor, S. C., & Binkowski, F. S. (2004). "An Analysis of the Time Scales Associated with Aerosol Processes During Dry Deposition". *Aerosol Science and Technology, 38*, 1091-1098.

Pryor, S. C., Gallagher, M., Sievering, H., Larsen, S. E., Barthelmie, R. J., Birsen, F., Vesala, T. (2008). "A Review of Measurement and Modelling Results of Particle Atmosphere Surface Exchange". *Tellus B: Chemical And Physical Meteorology, 60*(1), 42-75.

Pryor, S. C., Larsen, S. E., Sorensen, L. L., & Barthelmie, R. J. (2008). "Particle Fluxes Above Forests: Observations, Methodological Considerations, and Method Comparisons". *Environmental Pollutions, 152*, 667-678.

Pryor, S. C., Larsen, S. E., Sorensen, L. L., Barthelmie, R. J., Gronholm, T., Kulmala, M., Vesala, T. (2007). "Particle Fluxes Over Forests: Analyses of Flux Methods and Functional Dependencies". *Journal of Geophysical Research, 112*, D07205.

Reeks, M. W., & Hall, D. (2001). "Kinetic Models for Particle Resuspension in Turbulent Flows: Theory and Measurement". *Aerosol Science, 32*, 1-31.

Reeks, M. W., Reed, J., & Hall, D. (1988). "On the Resuspension of Small Particles by a Turbulent Flow". *Journal of Applied Physics, 21*, 574-589.

Ruijgrok, W., Tieben, H., & Eisinga, P. (1997). "The Dry Deposition of Particles to a Forest Canopy: A Comparison of Model and Experimental Results". *Atmospheric Environment, 31*(3), 399-415.

Schack, C. J., Sotiris, E. P., & Friedlander, S. K. (1985). "A General Correlation for Deposition of Suspended Particles from Turbulent Gases to Completely Rough Surfaces". *Atmospheric Environment, 19*, 983-1011.

Sehmel, G. A. (1970). "Particle Deposition from Turbulent Air Flow". *Journal of Geophysical Research, 75*(9), 1766-1781.

Sehmel, G. A. (1971). "Particle Diffusivities and Deposition Velocities over a Horizontal Smooth Surface". *Journal of Colloid and Interface Science, 37*(4), 891-906.

Sehmel, G. A. (1973). "Particle Eddy Diffusivities and Deposition Velocities for Isothermal Flow and Smooth Surfaces". *Aerosol Science, 4*, 125-138.

Sehmel, G. A., & Hodgson, W. H. (1978). *A Model for Predicting Dry Deposition of Particles and Gases to Environment Surfaces - PNL-SA-6721.* Richland: Battelle-Pacific Northwest Laboratories.

Seinfeld, J. H., & Pandis, S. N. (2012). *Atmospheric Chemistry and Physics: From Air Polution to Climate Change.* New York: John Wiley.

Simpson, M., Belles, R., & Gowardhan, A. (2013). *Improving NARAC Accuracy by Implementation of Higher-Resolution Precipitation and Deposition Modeling (LLNL-TR-643769).* Livermore, CA: Lawrence Livermore National Laboratory.

Simpson, M., Belles, R., & Walker, H. (2014). *Improving NARAC Accuracy by Implementation of Higher Resolution Precipitation and Deposition Modeling (LLNL-TR-660754).* Livermore, CA: Lawrence Livermore National Laboratory.

Simpson, M., Belles, R., & Walker, H. (2014). *Improving NARAC Accuracy by Implementation of Higher-Resolution Precipitation and Deposition Modeling (LLNL-TR-652474).* Livermore, CA: Lawrence Livermore National Laboratory.

Simpson, M., Belles, R., Fischer, K., & Walker, H. (2015). *Improving NARAC Accuracy by Implementation of Higher-Resolution Precipitation and Deposition Modeling (LLNL-TR-XXXXXX).* Livermore, CA: Lawrence Livermore National Laboratories.

Slinn, S. A., & Slinn, W. G. (1980). "Predictions for Particle Deposition on Natural Waters". *Atmospheric Environment, 14*, 1013-1016.

Slinn, W. G. (1982). "Predictions of Particle Deposition to Vegetative Surfaces". *Atmospheric Environment, 16*, 1785-1794.

Stein, A. D. (2015). "NOAA's HYSPLIT Atmospheric Transport and Dispersion Modeling System". *Bulletin of the American Meteorological Society, 96*, 2059-2077.

Stempniewicz, M. M., & Komen, E. M. (2010). "Comparison of Several Resuspension Models Against Measured Data". *Nuclear Engineering and Design, 240*, 1657-1670.

Stohl, A., Forster, C., Frank, A., Seibert, P., & Wotawa, G. (2005). "Technical Note: The Lagrangian Particle Dispersion Model FLEXPART version 6.2". *Atmospheric Chemistry and Physics, 5*, 2462-2474.

Stohl, A., Sodemann, H., Eckhardt, S., Frank, A., Seibert, P., & Watawa, G. (2010). *The Lagrangian Particle Dispersion Model FLEXPART version 8.2, User Manual.*

Terfous, A., Hazzab, A., & Ghenaim, A. (2013). "Predicting the Drag Coefficient and Settling Velocity of Spherical Particles". *Powder Technology, 239*, 12-20.

Tsakalakis, K. G., & Stamboltzis, G. A. (2001). "Prediction of the Settling Velocity of Irregularly Shaped Particles". *Minerals Engineering, 14*(3), 349-357.

Vainshtein, P., Ziskind, G., Fichman, M., & Gutfinger, C. (1997). "Kinetic Model of Particle Resuspension by Drag Force". *Physical Review Letters, 78*(3), 551-554.

Venkatram, A., & Pleim, J. (1999). "The Electrical Analogy does not Apply to Modeling Dry Deposition of Particles". *Atmospheric Environment, 33*, 3075-3076.

Wang, H.-C. (1990). "Effects of Inceptive Motion on Particle Detachment from Surfaces". *Aerosol Science and Technology, 13*(3), 386-393.

Wesely, M. L., Cook, D. R., Hart, R. L., & Speer, R. E. (1985). "Measurements and Parameterization of Particle Sulfur Deposition Over Grass". *Journal of Geophysical Research, 90*, 2131-2143.

Williams, R. M. (1982). "A Model for the Dry Deposition of Particles to Natural Water Surfaces". *Atmospheric Environment, 16*, 1933-1938.

Wiman, B. L., & Agren, G. I. (1985). "Aerosol Depletion and Deposition in Forests, A Model Analysis". *Atmospheric Environment, 19*, 335-362.

Wu, Y.-L., Davidson, C. I., Dolske, D. A., & Sherwood, S. I. (1992). "Dry Deposition of Atmospheric Contaminants: The Relative Importance of Aerodynamic, Boundary Layer, and Surface Resistances". *Aerosol Science and Technoloby, 16*, 65-81.

Xu, B., Huang, N., He, W., & Chen, Y. (2017). "Investigation on Terminal Velocity and Drag Coefficient of Particles with Different Shapes". *Fifteenth Asian Congress of Fluid Mechanics* (pp. 1-6). IOP Publishing.

Zhang, J., Shao, Y., & Huang, N. (2014). "Measurement of Dust Deposition Velocity in Wind-Tunnel Experiment". *Atmospheric Chemistry and Physics, 14*, 8869-8882.

Zhang, L. S., Gong, S., Padro, J., & Barrie, L. (2001). "A Size-Segregated Particle Dry Deposition Scheme for an Atmospheric Aerosol Module". *Atmospheric Environment, 35*, 549-560.

Zhang, L., & He, Z. (2014). "Technical Note: An Emperical Algorithm Estimating Dry Deposition Velocity of Fine, Coarse, and Giant Particles". *Atmospheric Chemistry and Physics, 14*, 3729-3737.

Zhu, D., Kuhns, H. D., Gillies, J. A., Etyemezian, V., Gertler, A. W., & Brown, S. (2011). "Inferring Deposition Velocities from Changes in Aerosol Size Distributions Downwind of a Roadway". *Atmospheric Environment, 45*, 957-966.

Ziskind, G., Fichman, M., & Gutfinger, C. (1995). "Resuspension of Particulates from Surfaces to Turbulent Flows - Review and Analysis". *Journal of Aerosol Science, 26*(4), 613-644.

Page Intentionally Blank

Page Intentionally Blank

DISTRIBUTION

1 U.S. Nuclear Regulatory Commission
Office of Nuclear Regulatory Research (RES)
Attn: John Tomon
MS C3A24M
Washington, D.C. 20555-0001

1 U.S. Nuclear Regulatory Commission
Office of Nuclear Regulatory Research (RES)
Attn: Jeffrey Kowalczik
MS 3WFN 9A12
Washington, D.C. 20555-0001

1 Pacific Northwest National Laboratory
Attn: Jeremy Rishel
PO Box 999
MS: J2-25
Richland, WA 99352

1	MS0791	Lainy Cochran	06631
1	MS0748	Randy Gauntt	06232
1	MS0736	Richard Griffith	06230
1	MS0748	John Fulton	06232
1	MS0791	Brian Hunt	06631
1	MS0791	Terry Kraus	06631
1	MS0791	Arthur Shanks	06631
1	MS0899	Technical Library	09536 (electronic copy)

Sandia National Laboratories